



**HAL**  
open science

## Population genomics revealed cryptic species within host-specific zombie-ant fungi (*Ophiocordyceps unilateralis*)

Noppol Kobmoo, Suchada Mongkolsamrit, Nuntanat Arnarnart, Janet Jennifer Luangsa-Ard, Tatiana Giraud

### ► To cite this version:

Noppol Kobmoo, Suchada Mongkolsamrit, Nuntanat Arnarnart, Janet Jennifer Luangsa-Ard, Tatiana Giraud. Population genomics revealed cryptic species within host-specific zombie-ant fungi (*Ophiocordyceps unilateralis*). *Molecular Phylogenetics and Evolution*, In press, 10.1016/j.ympev.2019.106580 . hal-02266424

**HAL Id: hal-02266424**

**<https://agroparistech.hal.science/hal-02266424>**

Submitted on 14 Aug 2019

**HAL** is a multi-disciplinary open access archive for the deposit and dissemination of scientific research documents, whether they are published or not. The documents may come from teaching and research institutions in France or abroad, or from public or private research centers.

L'archive ouverte pluridisciplinaire **HAL**, est destinée au dépôt et à la diffusion de documents scientifiques de niveau recherche, publiés ou non, émanant des établissements d'enseignement et de recherche français ou étrangers, des laboratoires publics ou privés.



Distributed under a Creative Commons Attribution - NonCommercial - NoDerivatives 4.0 International License

1 **Population genomics revealed cryptic species within host-specific zombie-ant fungi**

2 *(Ophiocordyceps unilateralis)*

3  
4 Noppol KOBMOO<sup>†,‡</sup>, Suchada MONGKOLSAMRIT<sup>†</sup>, Nuntanat ARNAMNART<sup>†</sup>, Janet Jennifer LUANGSA-ARD<sup>†</sup>,  
5 Tatiana GIRAUD<sup>‡</sup>

6 <sup>†</sup> National Center for Genetic Engineering and Biotechnology (BIOTEC), National Science and Technology  
7 Development Agency (NSTDA), 113 Thailand Science Park, Phahonyothin Rd., Khlong Nueng, Khlong Luang, 12120  
8 THAILAND.

9 <sup>‡</sup> Ecologie Systématique Evolution, Univ. Paris-Sud, CNRS, AgroParisTech, Université Paris-Saclay 91400 Orsay,  
10 France.

11  
12 Corresponding author: Noppol Kobmoo,

13 E-mail: [noppol.kob@biotec.or.th](mailto:noppol.kob@biotec.or.th)

14  
15 © 2019. This manuscript version is made available under CC-BY-NC-ND 4.0 license  
<http://creativecommons.org/licenses/by-nc-nd/4.0/>

28 **Abstract**

29 The identification and delimitation of species boundaries are essential for understanding speciation  
30 and adaptation processes and for the management of biodiversity as well as development for  
31 applications. *Ophiocordyceps unilateralis* sensu lato is a complex of fungal pathogens parasitizing  
32 Formicine ants, inducing zombie behaviors in their hosts. Previous taxonomic works with limited  
33 numbers of samples and markers led to the “one ant-one fungus” paradigm, resulting in the use of  
34 ant species as a proxy for fungal identification. Here, a population genomic study with sampling on  
35 three ant species across Thailand supported the existence of host-specific species in *O. unilateralis*  
36 s.l. with no footprints of long term introgression despite occasional host shifts and first-generation  
37 hybrids. We further detected genetic clusters within the previously delimited fungal species, with  
38 each little footprints of recombination, suggesting high levels of inbreeding. The clusters within  
39 each of *O. camponoti-leonardi* and *O. camponoti-saundersi* were supported by differentiation  
40 throughout the genome, suggesting they may constitute further cryptic species parasitizing the same  
41 host, challenging the one ant-one fungus paradigm. These genetic clusters had different  
42 geographical ranges, supporting different biogeographic influences between the north/center and the  
43 south of Thailand, reinforcing the scenario in which Thailand endured compartmentation during the  
44 latest Pleistocene glacial cycles.

45

46 Key words: *Ophiocordyceps unilateralis*, cryptic species, phylogenetic species, recombination, population genomics.

47

48

49

50

51

52

53

## 54 **1. Introduction**

55           The identification and delimitation of species boundaries are essential for understanding  
56 speciation and adaptation processes and for the management of biodiversity and conservation. The  
57 existence of cryptic species, i.e. distinct species with hardly distinguishable morphologies, have  
58 been increasingly documented in all phyla and constitutes a challenge for the study of speciation,  
59 the assessment of biodiversity and the implementation of conservation plans (Fišer et al., 2018;  
60 Struck et al., 2018). Particularly for fungi, the recognition of species can be difficult as they are  
61 versatile organisms, with variable morphology and life styles (Khonsanit et al., 2019; Molina et al.,  
62 2011; Mongkolsamrit et al., 2018; Montarry et al., 2009; Vincenot et al., 2017). Fungi are frequently  
63 symbionts to other organisms and often evolve host specialization (Fournier and Giraud, 2008;  
64 Gerardo et al., 2006, 2004), which is a fertile background for host-specific, cryptic species. The use  
65 of the phylogenetic species criterion based on concordance between gene genealogies has been  
66 highly useful for delimiting fungal cryptic species (Taylor et al., 2000). With the advent of next-  
67 generation sequencing, the concordance among gene genealogies can be assessed throughout the  
68 genome and new phylogenetic species can be revealed with even more power and reliability  
69 (Matute and Sepúlveda, 2019; Weiss et al., 2018) or well-established species can be questioned  
70 (Lifjeld, 2015). Furthermore, a population genomics approach can identify gene flow and  
71 introgression at fine scale along the genome (Chan et al., 2017; Savary et al., 2018).

72           *Ophiocordyceps unilateralis sensu lato* is a ubiquitous species complex of ant-pathogenic  
73 fungi with a pan-tropical distribution (Araújo et al., 2018) and an outstanding biology; these fungi  
74 modify the behavior of their ant hosts to promote their own dispersal. Infected ants are called  
75 zombie ants because they develop erratic behaviors, excluding themselves from their nest before  
76 climbing into vegetation and biting vegetal substrates until death (Hughes et al., 2011). The taxon  
77 called *O. unilateralis* has historically been characterized by the presence of fungal stalks arising  
78 from dead ants with lateral cushions containing perithecia and whole ascospores. Recent studies

79 based on morphology and molecular markers have shown that *O. unilateralis* represented a complex  
80 of cryptic species, with allopatric species from distinct continents (Araújo et al., 2018) as well as  
81 host-specific sympatric species (Kobmoo et al., 2012). A single and host-specific fungal species  
82 appeared to be associated to each ant species, leading to the “one ant-one fungus” paradigm and to  
83 the use of ant host identity as proxy for fungal species identification. However, little attention has  
84 been paid to intra-specific diversity and to the possibility of differentiated populations or species  
85 occurring on a given ant species. Species in the *O. unilateralis* complex are closely related and  
86 many are sympatric, which could lead to introgression and hybridization, although these questions  
87 have never been comprehensively studied.

88 In Thailand, six cryptic species of the *O. unilateralis s.l.* complex have been identified based  
89 on molecular phylogenies and morphological traits (Kobmoo et al., 2015; Luangsa-ard et al., 2011):  
90 *O. polyrhachis-furcata*, *O. camponoti-leonardi*, *O. camponoti-saundersi*, *O. septa* and *O. rami* and  
91 *O. halabalaensis*. At the macro-morphological level, only *O. rami* and *O. halabalaensis* can be  
92 easily distinguished from the others, having one stalk arising from the junction of the ant head and  
93 thorax, and two others arising from the junction of the forelegs and thorax; *O. rami* has sinuous  
94 purple stromata while *O. halabalaensis* has bigger but less sinuous blackish-brown stromata. At the  
95 micro-morphological level, *O. septa* has distinctive swollen and multi-septate ascospores; *O.*  
96 *polyrhachis-furcata*, *O. camponoti-leonardi* and *O. camponoti-saundersi* are the most similar  
97 genetically and morphologically and can be found on the ants *Polyrhachis furcata*, *Colobopsis*  
98 *leonardi* and *Colobopsis saundersi*, respectively (Kobmoo et al., 2012). Although morphological  
99 traits can distinguish these species, host species is the most convenient proxy for species  
100 identification and appears reliable (Araújo et al., 2018; Kobmoo et al., 2015, 2012). The criterion of  
101 congruence among gene genealogies was consistent with the separation of these host-specialized  
102 cryptic species in *O. unilateralis s.l.* (Kobmoo et al., 2012); however, they were based on only two  
103 gene sequences (Elongation factor 1-alpha and Beta tubulin).

104           Due to frequent expansion and contraction events of the forest during the Pleistocene glacial  
105 cycles, Southeast Asia shows strong biogeographic compartmentation (Woodruff, 2010). Genetic  
106 differentiation between the north and the peninsular south have been reported in many organisms,  
107 including insects such as bees (Insuan et al., 2007; Sittipraneed et al., 2001) and flies (Pramual et  
108 al., 2005), trees (Yu et al., 2019), vertebrates including frogs (Chen et al., 2018), monkeys (Karanth  
109 et al., 2008) and bats (Tu et al., 2017); so far this geographical pattern has not been studied in fungi.  
110 Furthermore, an increase in genetic diversity from North to South has been reported in various  
111 organisms in the Northern hemisphere, including fungi (Miraldo et al., 2016; Smith et al., 2017;  
112 Vercken et al., 2010) although investigations in Southeast Asia are still lacking.

113           Furthermore, genetic diversity in fungi is also influenced by reproductive modes (sexual vs  
114 clonal) and mating systems (selfing vs outcrossing) (Nieuwenhuis and James, 2016). The sexual  
115 reproductive structures of *O. unilateralis* has been widely observed in nature; the fungi develop  
116 ascomata from diseased ants, which release ascospores into the environment. However, additional  
117 transmission via conidia (asexual spores) cannot be ruled out and sexual reproduction can occur  
118 between closely related individuals, and even between clonemates in case these fungi are  
119 homothallic, which is unknown. Which reproductive mode and mating system are predominant, and  
120 whether there are differences between species, are still open questions which can have major  
121 implications for genetic diversity, reproductive barrier and adaptation in these fungi.

122           In the present study, we therefore used a population genomics approach to investigate: i)  
123 whether the existence of host-specific cryptic species was supported by genome-wide genetic  
124 differentiation in *O. unilateralis*, ii) in this case, whether introgression occurred between species,  
125 and in which genomic locations, iii) whether cryptic genetic subdivision could be identified beyond  
126 host specific species, e.g. according to geographic regions, iv) whether genetic diversity increased  
127 towards the South within each species, and v) what the reproductive mode and mating system of the  
128 different species were. For these goals, we collected samples of *O. polyrhachis-furcata*, *O.*

129 *camponoti-leonardi* and *O. camponoti-saundersi* (identified based on host identity as a first proxy)  
130 across Thailand, and sequenced their genomes. We investigated their species status using the  
131 criterion of concordance between genealogies performed using multiple genomic regions. We also  
132 studied the genetic subdivision within each species, possibly related to geography, as well as  
133 possible clines in diversity, and the possibility of introgression between species through analyses of  
134 Bayesian clustering and allelic spectrum-based models. Finally, we also searched for footprint of  
135 recombination to gain insight into the mode of reproduction.

136

## 137 **2. Materials and Methods**

### 138 **2.1 Sampling, isolation and sequencing**

139 A total of 59 samples of *O. unilateralis s.l.* were collected in Thailand, 29 on *C. leonardi*, 16  
140 on *C. saundersi* and 14 on *P. furcata* (Fig. 1a and Table 1S); fungal samples were named according  
141 to their host species (i.e., *O. polyrhachis-furcata*, *O. camponoti-leonardi* and *O. camponoti-*  
142 *saundersi*, respectively). To conform to the Nagoya protocols on access and benefit-sharing, we  
143 obtained an authorization from the Department of National Parks, Wildlife and Plant Conservation  
144 (DNP) at the Ministry of Natural Resources and Environment of Thailand for all strain collections.  
145 Isolations and extractions of fungal DNA were conducted following Kobmoo et al. (2018).  
146 Basically, ascospores were harvested after being discharged from the sexual reproductive structures  
147 (perithecia) of each sample on potato dextrose agar; whenever possible, random single ascospores  
148 were picked up with a needle and transferred to a liquid medium for culturing haploid strains. A  
149 single monospore strain per sample was retained for analyses. However, initiating cultures from  
150 single spores was not consistently successful; some strains were thus obtained by pooling the  
151 discharged ascospores together and thus result from a mixture of products of meiosis from a diploid  
152 individual; the corresponding DNAs thus correspond to diploid genotypes. Ascospores are thought  
153 to constitute the principal mode of infection for *O. unilateralis* (Araújo and Hughes, 2016) but it is

154 still unknown whether infections by two mating-type compatible haploid individuals are required to  
155 allow for sexual reproduction or whether these fungi are homothallic.

156 DNA quality and quantity were checked with gel electrophoresis using 0.8 % agarose gel and a  
157 Nanodrop (ThermoFisher). Paired-end genomic libraries (150 bp) were constructed and sequenced  
158 with an Illumina HiSeq3000 system at the GenoToul platform (Toulouse, France).

159

## 160 **2.2 Mapping and detection of single nucleotide polymorphisms**

161 The raw reads were trimmed for adaptors and low-quality bases on both ends ( $q < 20$ ) with  
162 Trim Galore! (Krueger, 2015). Reads shorter than 50 bp were discarded. Processed reads were then  
163 initially mapped to the latest version of *O. polyrhachis-furcata* reference (Kobmoo et al., 2018),  
164 thanks to its higher quality (43.25 Mb, 68 scaffolds, N50 ~ 2.9 Mb) compared to those of the two  
165 other species (*O. camponoti-leonardi*: 37.91 Mb, 531 scaffolds, N50 ~ 140 Kb; *O. camponoti-*  
166 *saundersi*: 49.26 Mb, 1,700 scaffolds, N50 ~ 102 Kb), using bwa-mem (Li, 2013) with the options -  
167 k 15 -d 150 -c 2000 -D 0.3 -B 1 -O 3 -Y -M. SNPs were detected using GATK (McKenna et al.,  
168 2010) through the GATK HaplotypeCaller function. The ploidy parameter was set as haploid for  
169 single-spore strains, and as diploid for multiple-spore strains as, for a given strain, a bulk of spores  
170 from the sample represents a mix of products of multiple meioses from the same diploid individual.  
171 As there were no reference variants, the variant recalibration step was dismissed but the variants  
172 were filtered *a posteriori* with total depth between 700x and 5000x, depth for individual samples >  
173 10, mapping quality > 10, quality normalized by depth > 20, genotyping quality > 50; various  
174 corrections for biases related to the difference of quality between reference and variant alleles were  
175 also applied. Any SNP overlapping with regions including repeats identified beforehand with  
176 RepeatMasker (Smit et al., <http://www.repeatmasker.org>) was excluded. Finally, only biallelic SNPs  
177 without indels and with at least 80% samples with reliable inferred variants were retained.

178 For the within-species analyses, the reads from *O. camponoti-leonardi* and *O. camponoti-*  
179 *saundersi* were mapped to their respective reference (Kobmoo et al., 2018). The same procedures of  
180 mapping and variant calling were applied as in *O. polyrhachis-furcata* above with slightly different  
181 filtering (for *O. camponoti-leonardi*, final SNPs with total depth between 50x and 3000x, mapping  
182 quality > 10, quality normalized by depth > 20; for *O. camponoti-saundersi*, final SNPs with total  
183 depth between 50x and 1000x, depth for individual samples > 20, mapping quality > 10, quality  
184 normalized by depth > 20).

185

### 186 ***2.3 Phylogenetic reconstruction and genealogical concordance phylogenetic species recognition*** 187 ***(GCPSR)***

188 Whole scaffold sequences for each sample were obtained using the  
189 *FastaAlternateReferenceMaker* tool in GATK. Sequences of a given scaffold from different samples  
190 altered at the SNPs positions were aligned using an in-house awk script. The alignments of all  
191 scaffolds were concatenated to generate a whole-genome alignment. The alignments were used to  
192 build maximum-likelihood phylogenetic trees with RaxML based on the model GTRCAT with 1000  
193 bootstrap replicates. A tree for each scaffold with variants was inferred with the same parameters.  
194 All trees were rooted with *O. kimflemingiae* (De Bekker et al., 2017), by aligning this latest genome  
195 to that of *O. polyrhachis-furcata* using the nucmer command from MUMmer 3 (Delcher, 2002;  
196 Kurtz et al., 2004). The concordance between different genomic regions was also evaluated under  
197 the framework of Bayesian concordance analyses using BUCKy v.1.4.4 (Larget et al., 2010), after  
198 Bayesian inferences over all scaffolds with SNPs bigger than 100 Kb chunked by 100 Kb separately  
199 using MrBayes 3.2.2 (Ronquist et al., 2012). The MCMC chains were allowed to sample across the  
200 substitution model space. Chunks of 100 Kb were used due to the high linkage disequilibrium found  
201 (see the section 3.7). The posterior tree distributions from the Bayesian inferences were fed into  
202 BUCKy to estimate the concordance of the nodes among the tree topologies, given as a

203 concordance factor (CF) ranging from 0 to 1 (absence of concordance to complete concordance).  
204 The concordance factor thus represents the genome-wide genealogical support for the monophyly of  
205 clades.

206

#### 207 ***2.4 Linkage disequilibrium, recombination footprints***

208 The correlation coefficient  $r^2$  between SNPs of less than 1M bp with minor allele frequency  
209 of at least 0.1 and per-sample inbreeding coefficients for diploid samples were calculated with plink  
210 (Purcell et al., 2007);  $r^2$  is a correlation coefficient representing the association and thus linkage  
211 between SNPs. In case of regular recombination, physically close SNPs are expected to be linked  
212 thus to have higher  $r^2$  than farther SNPs. In case of low frequency of sexual reproduction, linkage  
213 disequilibrium, and thus  $r^2$ , will be low across the whole genome. The  $r^2$  coefficient was averaged  
214 over 100 bp intervals and plotted against the pairwise physical distance to obtain linkage  
215 disequilibrium (LD) decay plots. Pairwise Homoplasmy Index (PHI) tests of recombination (Bruen et  
216 al., 2006) were performed for the whole dataset and for each species on each scaffold. The test is  
217 based on the detection of incompatibility between pairs of sites regarding whether there is a  
218 genealogical history that can be inferred parsimoniously that does not involve any convergent  
219 mutations; if any incompatibility exists, under an infinite-site model of evolution, it must come  
220 from recombination. PHI-test returns the probability of observing the data under the null hypothesis  
221 of no recombination. Bonferroni corrections were applied to the p-values. Population-scaled  
222 recombination rates ( $\rho = 2N_e \times r$ ;  $N_e$  = effective population size,  $r$  = recombination per site per  
223 generation) were calculated for each species using the R package FastEPRR (Gao et al., 2016). The  
224 per-sample inbreeding coefficients were calculated for diploid individuals as method-of-moments  
225 estimate F coefficients based on observed and expected homozygosity for each diploid sample.

226 Neighbor-net networks were inferred using SplitsTree (Huson and Bryant, 2006) for the whole  
227 dataset and for each species to gain insights into the level of recombination between and within the  
228 various *O. unilateralis* species.

229

### 230 **2.5 Principal component analysis (PCA), molecular diversity and genetic differentiation**

231 The nucleotide diversity ( $\pi$ ) of all species/populations and inter-specific/inter-population  
232  $F_{ST}$  and  $d_{xy}$  values were calculated using PopGenome package in R (Pfeifer et al., 2014). These  
233 calculations were performed based on SNPs called using the *O. polyrhachis-furcata* reference to use  
234 a common set of SNPs. The correlation between  $\pi$  and the latitude of the populations was tested  
235 with a Spearman's correlation test. We investigated the pattern of isolation by distance (IBD) by  
236 testing the existence of a correlation between  $F_{ST}/(1 - F_{ST})$  and the log of geographic distance  
237 (Rousset, 1997), using a Mantel test with 10,000 permutations.

238

### 239 **2.6 Genetic clustering, inference of gene flow and introgression**

240 A Bayesian clustering was conducted via FastStructure (Raj et al., 2014) with admixture  
241 model for the whole dataset to infer genetic structures between species. At the intra-specific level,  
242 we conducted the same analysis using the SNPs generated from each species reference. The most  
243 relevant number of clusters (K) were determined based on the plots of marginal likelihood and  
244 visual assessment of the barplots. The introgression footprints along the genome were investigated  
245 with a clustering analysis of genetic similarity on 500 SNPs sliding windows among the samples  
246 based on Gower's distance, using Mclust package in R (Scrucca et al., 2016). Neighbor-joining  
247 trees based on the F84 distance (Kishino and Hasegawa, 1989)(Kishino and Hasegawa, 1989) were  
248 also constructed to illustrate the relationships among the different clusters.

249 To infer events of gene flow between species, we used TreeMix (Pickrell and Pritchard,  
250 2012) which estimates the most likely topology representing the evolutionary history between

251 populations and mixing based on genome-wide allele frequency data. TreeMix compares the  
252 likelihood of models with different numbers of migration events between populations.

253

### 254 **3. Results**

#### 255 **3.1 Detection of single nucleotide polymorphisms (SNPs)**

256 By using *O. polyrhachis-furcata* BCC54312 as the reference for mapping all genomes, we  
257 retained 688,264 SNPs in the whole dataset. Only a small proportion of them was shared between  
258 the three host species (1144 SNP ~ 0.166 %, Fig.S1). Based on the phylogenetic species recognition  
259 analysis (see the subsection 3.2), we excluded a sample from the host *C. leonardi* with an unclear  
260 placement (NK122ss). There were 443,670 SNPs in the remaining dataset. The samples classified  
261 as *O. camponoti-leonardi* had more SNPs (219,017) than the other species (92,133 for *O.*  
262 *camponoti-saundersi* and 53,552 for *O. polyrhachis-furcata*). By using the *O. polyrhachis-furcata*  
263 reference genome to detect SNPs in all species, we could expect to find higher diversity in *O.*  
264 *polyrhachis-furcata* due to a bias favoring detection of SNPs from this species. However, we  
265 observed in contrast fewer SNPs in *O. polyrhachis-furcata*, which is likely due to genuine lower  
266 genetic diversity in this species (see section 3.4). When using their respective references to call  
267 SNPs within each species, we found as expected more SNPs than when using the *O. polyrhachis-*  
268 *furcata* reference in the two other species (1,301,966 SNPs for *O. camponoti-leonardi* and 159,449  
269 SNPs for *O. camponoti-saundersi*).

270

#### 271 **3.2 Species delimitation using the phylogenetic criterion of species recognition**

272 The maximum likelihood (ML) tree based on whole genomes supported the existence of the  
273 three host-specific species. Indeed, we found three clades supported by 100% bootstrap support  
274 corresponding to the three hosts sampled (Fig.2a). The only exceptions were NK604, isolated from  
275 a *C. saundersi* ant but placed within the *O. camponoti-leonardi* clade, and NK122ss, isolated from

276 *C. leonardi* but placed as a sister group to the *O. camponoti-saundersi* clade with full bootstrap  
277 support (Fig.2a). The trees inferred from the different scaffolds displayed congruent topologies  
278 (Fig.2b) except for the scaffolds 6.2, 16, 18, 20, 21, 25, 29, 36, 41, 53, 105 (Fig.S2). Some of these  
279 scaffolds however suffered from a lack of polymorphism and/or yielded trees with low bootstrap  
280 supports (Table 2S).

281 The Bayesian concordance analysis comparing topologies between genealogies built from  
282 100 kb fragments showed high concordance factors (CFs above 0.9; Fig. 3a), further indicating that  
283 most genomic regions supported the three host-specific clades and thus the existence of distinct,  
284 host-specialized species. The Bayesian concordance analysis also confirmed the position of  
285 NK122ss as the sister group of *O. camponoti-saundersi* (Fig. 3a).

286

### 287 **3.3 Inter and intra-specific genetic differentiation**

288 Based on the SNPs inferred using *O. polyrhachis-furcata* as the reference, the Bayesian  
289 clustering also yielded clusters grouping samples according to host species, except again for NK604  
290 (Fig.1c). The sample NK122ss, from the host *C. leonardi*, had admixed membership up to K=4 but  
291 gained a total membership to a distinct cluster from K=5, where two other clusters were  
292 distinguished in this host (Fig.S3a), a pattern corroborated by PCA (Fig.1b). The sample NK122ss  
293 may belong to a species different from *O. camponoti-leonardi*, as also suggested by the  
294 phylogenies, and was thus excluded from further analyses. No additional cluster was found at  
295 higher Ks (Fig.S3a). The marginal likelihood curve in fact reached a plateau at K = 5 (Fig.S3b). The  
296 sample NK604, isolated from the host *C. saundersi*, clustered with those from the host *C. leonardi*  
297 in the PCA (Fig.1b), in agreement with the results on species delimitation, and was thus considered  
298 to belong to *O. camponoti-leonardi* in the following analyses. It is likely a spill over, i.e. an  
299 occasional infection from a non-endemic species without sustainable persistence. Furthermore, two  
300 genetic clusters could be clearly distinguished within *O. camponoti-leonardi* (OCL1 and OCL2 in

301 Fig.S1b and 1c). The genetic differentiation between the three main species was high ( $F_{ST} > 0.5$ ,  
 302 Table 1).

303

304 Table 1. Genetic differentiation between species ( $F_{ST}$ : above the diagonal,  $d_{xy}$ : below the diagonal;  
 305 OCL = *Ophiocordyceps camponoti-leonardi*, OCS = *O. camponoti-saundersi*, OPF = *O.*  
 306 *polyrhachis-furcata*). The nucleotide diversity ( $\Pi$ ) within species is given in the diagonal in bold;  
 307  $d_{xy}$  = absolute divergence between two species;  $F_{ST}$  = fixation index measuring relative divergence.

$F_{ST}$	OCL	OCS	OPF	<i>Ophiocordyceps</i> sp. nov. (NK122ss)
$d_{xy}$				
OCL	<b>0.026</b>	0.696	0.588	0.865
OCS	0.224	<b>0.015</b>	0.771	0.902
OPF	0.127	0.162	<b>0.007</b>	0.959
<i>Ophiocordyceps</i> <i>sp. nov.</i> (NK122ss)	0.309	0.269	0.257	<b>0</b>

308

309 We inferred genetic clusters within each of the three main species based on SNPs called  
 310 using specific reference per species. For *O. camponoti-leonardi*, the results were slightly different  
 311 from those when the *O. polyrhachis-furcata* reference was used (see above), as we retrieved three  
 312 clusters (OCL1, OCL2, OCL3) for most K values (Fig.4a and Fig.S4a). Only at K=6 were four  
 313 clusters observed but the fourth disappeared at higher K values and the marginal likelihood was  
 314 lowest at K=6 (Fig.S4b). We therefore considered three genetic clusters in *O. camponoti-leonardi*;  
 315 two clusters were parapatric—one in the extreme North (OCL1) and another one extended to the  
 316 center (OCL2). The samples NK140 and NK561, which appeared to belong to OCL2 using SNPs  
 317 called with the *O. polyrhachis-furcata* reference (Fig.1b and 1c), were assigned differently when  
 318 using SNPs called with the *O. camponoti-leonardi* reference; the sample NK140 displayed an

319 admixed genetic membership but still mostly belonged to OCL2 while the sample NK561 from the  
 320 south of Thailand was assigned to another cluster (OCL3).  
 321 Regarding *O. camponoti-saundersi*, three sympatric clusters (OCS1, OCS2, OCS3) were found  
 322 from K=3 and above, with a plateau reached at K=3 for the marginal likelihood (Fig. S5); the three  
 323 clusters were localized mainly in the north-east of Thailand (Fig. 4b). For *O. polyrhachis-furcata*,  
 324 the marginal likelihood oscillated between K=2 and K=10 (Fig. S6b); we identified three main  
 325 genetic clusters, one in the north-east of Thailand (OPF1) and two in the South (OPF2 and OPF3),  
 326 OPF3 being however represented by a single strain (NK157) (Fig. 4c and Fig. S6a). Another  
 327 individual from the South of Thailand (NK151) had different cluster assignments across the various  
 328 K values (Fig.4c and Fig.S6a). NJ trees and PCAs retrieved the same patterns of genetic  
 329 subdivisions within each of the three species (Fig.S7 - S9). The intra-specific differentiation level  
 330 (between clusters of a given named species) was overall slightly lower than inter-specific  
 331 differentiation level (Table 2).

332

333 Table 2. Genetic differentiation between genetic clusters ( $F_{ST}$ : above the diagonal,  $d_{xy}$ : below the  
 334 diagonal). The nucleotide diversity ( $P_i$ ) within clusters are given in the diagonal in bold. OCL3  
 335 includes a single individual (NK561).

Fst	OCL1	OCL2	OCL3	OCS1	OCS2	OCS3	OPF1	OPF2
$d_{xy}$								
OCL1	<b>0.011</b>	0.711	0.907	0.934	0.915	0.904	0.884	0.870
OCL2	0.144	<b>0.016</b>	0.781	0.877	0.853	0.841	0.749	0.736
OCL3	0.175	0.117	<b>0</b>	0.996	0.976	0.962	0.985	0.966
OCS1	0.262	0.216	0.246	<b>0.001</b>	0.913	0.834	0.979	0.962
OCS2	0.261	0.214	0.244	0.079	<b>0.010</b>	0.813	0.947	0.931
OCS3	0.268	0.221	0.250	0.063	0.081	<b>0.006</b>	0.927	0.912
OPF1	0.159	0.110	0.144	0.155	0.152	0.159	<b>0.001</b>	0.425
OPF2	0.164	0.116	0.149	0.161	0.158	0.165	0.013	<b>0.003</b>

336

### 337 **3.4 Nucleotide diversity and isolation by distance**

338 We used the SNPs inferred using the best assembled reference genome (*O. polyrhachis-*  
339 *furcata*) to compute nucleotide diversity ( $P_i$ ) to compare between species (Table 1) as well as  
340 between intra-specific clusters (Table 2). The nucleotide diversity was highest for *O. camponoti-*  
341 *leonardi* (0.026), followed by *O. camponoti-saundersi* (0.015) and *O. polyrhachis-furcata* (0.007).  
342 Based on the Bayesian clustering, we considered *O. camponoti-leonardi* to be composed of two  
343 genetic clusters, OCL1 and OCL2 (excluding the strain NK561 that appeared to belong to a distinct  
344 cluster; Fig. S4a and S7), *O. camponoti-saundersi* to be composed of three genetic clusters (OCS1,  
345 OCS2 and OCS3), and *O. polyrhachis-furcata* to be composed of two clusters (OPF1 and OPF2),  
346 excluding the two genetically distant individuals NK151 and NK157. The genetic diversity was  
347 variable among genetic clusters within each species ( $P_i$  values in Table 2). OCS1 had much lower  
348 diversity compared to OCS2 and OCS3, as shown by the  $P_i$  values and the shorter branches on the  
349 NJ tree (Fig. S8a). The correlation between genetic diversity ( $P_i$ ) and latitude for *O. camponoti-*  
350 *leonardi* was not significant (Spearman's correlation test:  $r = -0.3$ ,  $p$ -value = 0.683; Table 3S and  
351 Fig. 10Sa). Isolation by distance was not significant in *O. camponoti-leonardi* (Mantel's test:  $r =$   
352 0.236,  $p$ -value = 0.25; Fig.10Sb). Not enough sampling sites were available for the other species to  
353 test for such correlations.

354

### 355 **3.5 Concordance among genealogies for within-species clusters**

356 We then investigated whether the different clusters found within each of the identified  
357 cryptic species so far could be considered as distinct species based on the criterion of concordance  
358 among multiple genomic genealogies. The Bayesian concordance analysis based on 100-kb DNA  
359 fragments showed that the three clusters in *O. camponoti-saundersi* formed respectively clades with  
360 high CFs (above 0.85; Fig. 3b). For *O. camponoti-leonardi*, the clade OCL1 was strongly supported  
361 with a high CF (0.993) while the clade OCL2 as defined previously was poorly supported (CF =

362 0.477; OCL2 *sensu lato* in Fig.3b). However, when excluding NK140 from OCL2, the clade  
363 became strongly supported (CF = 0.901), while NK140, like NK561 which was previously shown  
364 to be admixed, had unclear status. For *O. polyrhachis-furcata*, the clusters OPF1 and OPF2 formed  
365 each a monophyletic clade but with low CFs (0.433 and 0.485 respectively: Fig.3b). Neighbor-net  
366 networks using SplitsTree also recovered different species (Fig.5) and the same well differentiated  
367 genetic clusters within species (Fig.S11).

368

### 369 **3.6 Introgression and gene flow between species**

370 Previous analyses showed that a few individuals had admixed genetic membership. We  
371 therefore performed genetic clustering analyses along the genome to identify possible footprints of  
372 localized introgression. The general pattern of host-specific clusters was found throughout the  
373 genome (Fig.6). However, introgression footprints was found along the genome for two individuals,  
374 NK151 and NK157, that showed admixed or distinct membership in comparison to the other *O.*  
375 *polyrhachis-furcata* samples in Bayesian clustering. The *O. camponoti-leonardi* individual NK561  
376 appeared here highly admixed between OCL1 and OCL2. We did not recover in this analysis the  
377 different genetic clusters in *O. camponoti-saundersi* (Fig.6). The Gower's genetic distance on which  
378 this clustering is based may not be able to detect finer genetic differences. Splitstree analyses  
379 recovered the same well differentiated genetic clusters within species and without footprints of  
380 extensive gene flow, except perhaps between OPF1 and OPF2 (Fig.S11).

381 Gene flow events were inferred using Treemix based on the allelic frequency spectra of the  
382 different species and clusters retrieved from the SNPs called on the *O. polyrhachis-furcata*  
383 reference genome. We excluded the individual with unclear status, i.e., NK122ss. To account for  
384 linkage disequilibrium, blocks of 500 SNPs were used. Setting the number of migration events to  
385 one, we inferred one gene flow event between OCL1 and OCS (Fig.7). However, the model with

386 gene flow was not significantly more likely than the model without migration (log likelihood ratio  
387 test: p-value 0.235).

388

### 389 **3.7 Linkage disequilibrium and recombination footprints**

390 We investigated recombination footprints within species and genetic clusters by looking at  
391 linkage disequilibrium (LD) decay (Fig.8). None of the species had their LD decaying to less than  
392 0.2 at the distance of 1 Mb, and the LD of both *O. camponoti-leonardi* and *O. camponoti-saundersi*  
393 remained flat after an initial rapid decrease, resembling patterns in clonal species (Sepúlveda et al.,  
394 2017). Using half of the maximum LD as the criteria for linkage distance (Taylor et al., 2015), *O.*  
395 *unilateralis* species seemed to maintain linkage over more than 1 Mb. Nevertheless, the PHI-tests  
396 revealed significant deviations from the expectation of no recombination for most scaffolds in *O.*  
397 *camponoti-leonardi* and *O. saundersi*, and their respective intra-specific genetic clusters. Evidence  
398 of recombination was found on fewer scaffolds for *O. polyrhachis-furcata*, both when considering  
399 the whole species and considering separately its intra-specific clusters (Table S4). For all species  
400 and their clusters, no footprints of recombination could be recovered from small scaffolds with little  
401 polymorphism (Table S4). The population-scaled recombination rates ( $\rho$ ) were all of similar order  
402 of magnitude ( $1.88e-5$  for *O. polyrhachis-furcata*,  $1.49e-5$  for *O. camponoti-leonardi* and  $5.95e-5$   
403 for *O. camponoti-saundersi*). Splitstree analyses also suggested low levels of recombination within  
404 species (Fig.4) and within genetic clusters (Fig.S11); reticulations were observed but seemed  
405 overall limited compared to the whole network except for *O. polyrhachis-furcata*, in which the  
406 reticulations appeared to be restricted to the two admixed samples (NK151 and NK157) (Fig.S11b).  
407 The per-sample inbreeding coefficients of the diploid samples were extremely high in all species,  
408 approaching 1; this means that most sites were homozygous (Table.S5), suggesting a very high level  
409 of inbreeding.

410

## 411 **4. Discussion**

### 412 **4.1 Host-specific species with occasional host-jump and gene flow**

413 Our population genomics study on Thai populations of *O. unilateralis sensu lato* from three  
414 ant hosts showed that, apart from a few exceptions, fungal species matched ant species. The  
415 previous separation of host-specific species within *O. unilateralis s.l.* from Thailand (*O. camponoti-*  
416 *leonardi*, *O. camponoti-saundersi* and *O. polyrhachis-furcata*) had strong whole-genome support  
417 with different methods, i.e., Bayesian clustering, PCA, maximum likelihood bootstrap and Bayesian  
418 concordance factors (BCF). In particular, the tree topologies obtained based on different genomic  
419 regions were congruent and supported the monophyly of individuals parasitizing a given host  
420 species, indicating that the three species *O. camponoti-leonardi*, *O. camponoti-saundersi* and *O.*  
421 *polyrhachis-furcata* form distinct lineages under the phylogenetic species criterion.

422 Nevertheless, one individual was found in an ant species different from the typical host of its  
423 species, as previously documented (Kobmoo et al., 2012), and two others showed signals of genetic  
424 admixture in Bayesian clustering which were also reflected into ambiguous or poorly supported  
425 placements in phylogenetic trees. Using an allelic frequency spectrum-based inference, a single  
426 event of gene flow from *O. camponoti-leonardi* to *O. camponoti-saundersi* was detected; however,  
427 the model with gene flow was not statistically more likely than the model without gene flow.  
428 Occasional spill-over or hybridization thus did not seem to lead to long term introgression among  
429 species, potentially due to selection against hybrids.

430

### 431 **4.2 Possible additional cryptic species and the one ant-one fungus paradigm**

432 Our population genomics study further revealed the existence of differentiated genetic  
433 clusters within each host-specific species. The clusters within *O. camponoti-leonardi* and *O.*  
434 *camponoti-saundersi* were particularly well differentiated and supported through different analyses,  
435 with little footprints of gene flow. Multiple genealogies were congruent in separating the genetic

436 clusters within *camponoti-saundersi* and *O. camponoti-leonardi* indicating they should be  
437 considered as distinct species according to the GCPSR criterion (Taylor et al., 2000), and not just as  
438 different populations, and they would deserve further morphological examinations in future studies.  
439 The clusters within *O. polyrhachis-furcata* in contrast did not appear supported as distinct species.

440 This study thus revealed hidden diversity beyond well described species, which could not be  
441 detected previously (Kobmoo et al., 2015, 2012), probably due to the limited quantity of markers  
442 and examined samples (Balasundaram et al., 2015; Taylor et al., 2000). In addition, a sample  
443 (NK122ss) did not cluster with other individuals parasitizing the same host species and was instead  
444 placed as a sister taxon to *O. camponoti-saundersi*, without presenting admixture footprints,  
445 suggesting that it could belong to a different species or be admixed with another species not present  
446 in the sample.

447 The finding that there could be more than one *Ophiocordyceps* species parasitizing a given  
448 host challenges the well-accepted “one ant-one fungus” paradigm (Araújo et al., 2018). It should  
449 however be noted that the ant taxonomy is itself still debated. The ants *Colobopsis leonardi* and *C.*  
450 *saundersi* were previously classified in the genus *Camponotus* before a recent resurrection of the  
451 genus *Colobopsis* (Ward et al., 2016) and both are cryptic species with unclear taxonomy (Laciny et  
452 al., 2018). The genetic clusters found within described *Ophiocordyceps* species in our study could  
453 actually be associated to different ant species in agreement with the one ant-one fungus hypothesis.  
454 A taxonomic work with a strong population genomics aspect on both the hosts and the parasites will  
455 be necessary to elucidate species delimitation and cophylogeny analyses to assess whether co-  
456 divergence occurred (De Vienne et al., 2013; Morand et al., 2015).

457

#### 458 **4.3 Reproductive mode and mating system in *Ophiocordyceps unilateralis***

459 Recombination likely occurs in *O. unilateralis* sensu lato, but probably very rarely. The rho  
460 values were of the same order of magnitude (-5) for all three host-specific species and much lower

461 than in fungi with regular outcrossing such as the heterothallic *Zymoseptoria tritici* and *Z. ardabilae*  
462 (rho values being respectively 0.0217 and 0.0045: Stukenbrock and Dutheil, 2018), or other fungi  
463 with diploid-selfing obligate sexual reproduction like *Microbotryum* species (order of magnitude -3  
464 to -2: Badouin et al., 2017) and *Saccharomyces paradoxus* (0.001 – 0.003: Tsai et al., 2008). The  
465 per-sample inbreeding coefficients for the diploid individuals were actually all very high in all  
466 species and clusters, indicating that most SNPs were homozygous. As all the strains used in this  
467 study were isolated from sexual spores resulting from meiosis, *O. unilateralis* regularly undergoes  
468 sexual reproduction. Altogether, these findings suggest for the whole species complex a high level  
469 of inbreeding or even frequent intra-haploid mating, i.e. mating between genetically identical  
470 haploid cells (Billiard et al., 2012; Giraud et al., 2008). Intra-haploid mating is only possible in  
471 homothallic fungi as the existence of mating types in heterothallic fungi prevents such mating.  
472 Whether *O. unilateralis* is homothallic or heterothallic is still unclear; the genome of *O.*  
473 *polyrhachis-furcata* contains at least a mating type locus (MAT-1-2) and a putative mating type-  
474 switching gene (Wichadakul, unpublished data) which suggests that it may be homothallic but no  
475 experimental observation has been done.

476         Such high inbreeding is consistent with the life history traits of these fungi. Fungal  
477 development into the transmission stage inside ant nest was not observed and infection outside the  
478 nest is likely favored to avoid social immunity (Loreto et al., 2014). Field observations and a  
479 theoretical model established that effective infections were rare; only a weak proportion of samples  
480 observed on field went through sexual reproduction (Andersen et al., 2012; Mongkolsamrit et al.,  
481 2012). The probability to encounter compatible spores from distinct diploid fungal individuals may  
482 be low, thus promoting selfing in the fungi. Low probability of outcrossing can be found in other  
483 pathogenic fungi such as the plant castrating anther-smut fungi *Microbotryum* in which mating  
484 occurs between cells resulting from the same meiosis issued from a dispersing diploid spore (Giraud  
485 et al., 2008; Vercken et al., 2010). The infective spores of *O. unilateralis* are haploid which could

486 render the probability to find a compatible mate in an insect even lower, favoring intra-haploid  
487 mating.

488

#### 489 **4.4 The biogeography of *Ophiocordyceps unilateralis* in Thailand**

490 While the genetic clusters detected within *O. camponoti-saundersi* were sympatric and all  
491 restricted to the Northeast of Thailand, *O. camponoti-leonardi* and *O. polyrhachis-furcata* had  
492 widely distributed genetic clusters, with different geographical ranges, mainly reflecting the  
493 separation between the north/center and the south of Thailand. Such genetic differentiation between  
494 the North and the South of Thailand has been documented in many organisms (Chen et al., 2018;  
495 Karanth et al., 2008; Pramual et al., 2005; Sittipraneed et al., 2001; Tu et al., 2017; Yu et al., 2019),  
496 which was suggested to reflect different biogeographic entities, one from the Indochina and another  
497 from the Malay peninsula (Woodruff, 2010). The existence of northern and southern distinct  
498 biogeographic compartments also explains that the genetic diversity does not increase toward south,  
499 contrary to what is found in the northern hemisphere for many organisms (Hewitt, 2012). Enlarging  
500 the sampling of both the hosts and the pathogens across Southeast Asia would give novel insights  
501 into the host-pathogen phylogeography of this region.

502

#### 503 **5. Conclusion**

504 In this study, population genomics supported the host-specificity of previously described  
505 cryptic species in ant pathogenic fungi and further revealed genetic clusters sharing the same host  
506 but with contrasting geographical ranges as candidates to be erected as new species in the zombie  
507 ant fungal complex *O. unilateralis* sensu lato. Whole genome analyses also revealed individuals  
508 with admixed genetic membership but not leading to persistent gene flow among species or genetic  
509 clusters. The recognition of cryptic species has direct impacts on species diversity assessment and  
510 ecological research and population genomics can be powerful to reveal hidden diversity, as shown

511 in our study. More generally, population genomics can reveal the existence of cryptic species or  
512 different populations of pathogens, contributing to our understanding of host-parasite/pathogen  
513 specificity and phylogeography. Furthermore, we studied for the first time recombination footprints  
514 in *O. unilateralis* sensu lato which suggested limited recombinations and a high level of inbreeding.

515

## 516 **Acknowledgements**

517 We would like to thank Alodie Snirc for advice concerning DNA extraction, Antoine Branca for  
518 help with bioinformatic protocols; Kanoksri Tasanathai, Donnaya Thanakitpipattana, Wasana  
519 Noisripoom and Artit Khonsanit for help in samples collection; Navavit Ponganan for making the  
520 maps in this publication. We also thank the Department of National Parks, Wildlife and Plant  
521 Conservation of Thailand for their cooperation and support of our project.

522

523 Funding: This work was supported by a Marie-Skłodowska Curie Action [grant number 655278] to  
524 NK, a Biotec Fellow's Research Grant [grant number P1950231] to J.J.L., and by the National  
525 Science and Technology Development Agency, Cluster and Program Management Office [grant  
526 number P1300854] to S.M.

527

## 528 **Supplementary Materials**

529 Supplementary Figures.

530 Table S1: Fungal isolates used in this study.

531 Table S2: Genetic diversity per scaffold in *Ophiocordyceps unilateralis sensu lato*.

532 Table S3: Genetic diversity by site and by species.

533

## 534 **Research Data**

535 The raw reads in this study were deposited at the NCBI Sequence Read Archive (SRA) under the  
536 accession PRJNA530395. The information regarding the fungal isolates used in this study were  
537 deposited at the NCBI BioSample under the accessions reported in the table S1 of the  
538 Supplementary Materials. The final sets of SNPs are available at...

539

## 540 **References**

- 541 Andersen, S.B., Ferrari, M., Evans, H.C., Elliot, S.L., Boomsma, J.J., Hughes, D.P., 2012. Disease  
542 dynamics in a specialized parasite of ant societies. *PLoS One* 7.  
543 <https://doi.org/10.1371/journal.pone.0036352>
- 544 Araújo, J.P.M., Evans, H.C., Kepler, R., Hughes, D.P., 2018. Zombie-ant fungi across continents: 15  
545 new species and new combinations within *Ophiocordyceps*. I. Myrmecophilous hirsutelloid  
546 species. *Stud. Mycol.* 90, 119–160. <https://doi.org/10.1016/j.simyco.2017.12.002>
- 547 Araújo, J.P.M., Hughes, D.P., 2016. Diversity of Entomopathogenic Fungi. Which Groups  
548 Conquered the Insect Body? *Adv. Genet.* 94, 1–39.  
549 <https://doi.org/10.1016/bs.adgen.2016.01.001>
- 550 Badouin, H., Gladieux, P., Gouzy, J., Siguenza, S., Aguilera, G., Snirc, A., Le Prieur, S., Jeziorski,  
551 C., Branca, A., Giraud, T., 2017. Widespread selective sweeps throughout the genome of  
552 model plant pathogenic fungi and identification of effector candidates. *Mol. Ecol.* 26, 2041–  
553 2062. <https://doi.org/10.1111/mec.13976>
- 554 Balasundaram, S. V., Engh, I.B., Skrede, I., Kausrud, H., 2015. How many DNA markers are  
555 needed to reveal cryptic fungal species? *Fungal Biol.* 119, 940–945.  
556 <https://doi.org/10.1016/j.funbio.2015.07.006>
- 557 Billiard, S., López-Villavicencio, M., Hood, M.E., Giraud, T., 2012. Sex, outcrossing and mating  
558 types: Unsolved questions in fungi and beyond. *J. Evol. Biol.* <https://doi.org/10.1111/j.1420-9101.2012.02495.x>
- 560 Bruen, T.C., Philippe, H., Bryant, D., 2006. A simple and robust statistical test for detecting the  
561 presence of recombination. *Genetics* 172, 2665–2681.  
562 <https://doi.org/10.1534/genetics.105.048975>
- 563 Chan, K.O., Alexander, A.M., Grismer, L.L., Su, Y.-C., Grismer, J.L., Quah, E.S.H., Brown, R.M.,  
564 2017. Species delimitation with gene flow: A methodological comparison and population  
565 genomics approach to elucidate cryptic species boundaries in Malaysian Torrent Frogs. *Mol.*  
566 *Ecol.* 26, 5435–5450. <https://doi.org/10.1111/mec.14296>
- 567 Chen, J.M., Poyarkov, N.A., Suwannapoom, C., Lathrop, A., Wu, Y.H., Zhou, W.W., Yuan, Z.Y., Jin,  
568 J.Q., Chen, H.M., Liu, H.Q., Nguyen, T.Q., Nguyen, S.N., Duong, T. Van, Eto, K., Nishikawa,  
569 K., Matsui, M., Orlov, N.L., Stuart, B.L., Brown, R.M., Rowley, J.J.L., Murphy, R.W., Wang,

- 570 Y.Y., Che, J., 2018. Large-scale phylogenetic analyses provide insights into unrecognized  
571 diversity and historical biogeography of Asian leaf-litter frogs, genus *Leptotalax* (Anura:  
572 Megophryidae). Mol. Phylogenet. Evol. 124, 162–171.  
573 <https://doi.org/10.1016/j.ympev.2018.02.020>
- 574 De Bekker, C., Ohm, R.A., Evans, H.C., Brachmann, A., Hughes, D.P., 2017. Ant-infecting  
575 *Ophiocordyceps* genomes reveal a high diversity of potential behavioral manipulation genes  
576 and a possible major role for enterotoxins. Sci. Rep. 7, 1–13. <https://doi.org/10.1038/s41598-017-12863-w>  
577
- 578 De Vienne, D.M., Refrégier, G., López-Villavicencio, M., Tellier, A., Hood, M.E., Giraud, T., 2013.  
579 Cospeciation vs host-shift speciation: Methods for testing, evidence from natural associations  
580 and relation to coevolution. New Phytol. 198, 347–385. <https://doi.org/10.1111/nph.12150>
- 581 Delcher, A.L., 2002. Fast algorithms for large-scale genome alignment and comparison. Nucleic  
582 Acids Res. 30, 2478–2483. <https://doi.org/10.1093/nar/30.11.2478>
- 583 Fišer, C., Robinson, C.T., Malard, F., 2018. Cryptic species as a window into the paradigm shift of  
584 the species concept. Mol. Ecol. 27, 613–635. <https://doi.org/10.1111/mec.14486>
- 585 Fournier, E., Giraud, T., 2008. Sympatric genetic differentiation of a generalist pathogenic fungus,  
586 *Botrytis cinerea*, on two different host plants, grapevine and bramble. J. Evol. Biol. 21, 122–  
587 132. <https://doi.org/10.1111/j.1420-9101.2007.01462.x>
- 588 Gao, F., Ming, C., Hu, W., Li, H., 2016. New Software for the Fast Estimation of Population  
589 Recombination Rates (FastEPRR) in the Genomic Era. G3 Genes|Genomes|Genetics 6, 1563–  
590 1571. <https://doi.org/10.1534/g3.116.028233>
- 591 Gerardo, N.M., Jacobs, S.R., Currie, C.R., Mueller, U.G., 2006. Ancient host-pathogen associations  
592 maintained by specificity of chemotaxis and antibiosis. PLoS Biol. 4, 1358–1363.  
593 <https://doi.org/10.1371/journal.pbio.0040235>
- 594 Gerardo, N.M., Mueller, U.G., Price, S.L., Currie, C.R., 2004. Exploiting a mutualism: Parasite  
595 specialization on cultivars within the fungus-growing ant symbiosis. Proc. R. Soc. B Biol. Sci.  
596 271, 1791–1798. <https://doi.org/10.1098/rspb.2004.2792>
- 597 Giraud, T., Yockteng, R., López-Villavicencio, M., Refrégier, G., Hood, M.E., 2008. Mating system  
598 of the anther smut fungus *Microbotryum violaceum*: Selfing under heterothallism. Eukaryot.  
599 Cell. <https://doi.org/10.1128/EC.00440-07>
- 600 Hewitt, G.M., 2012. Quaternary Genetic consequences of climatic oscillations in the Genetic  
601 consequences of climatic oscillations in the Quaternary. <https://doi.org/10.1098/rstb.2003.1388>
- 602 Hughes, D.P., Andersen, S.B., Hywel-Jones, N.L., Himaman, W., Billen, J., Boomsma, J.J., 2011.  
603 Behavioral mechanisms and morphological symptoms of zombie ants dying from fungal  
604 infection. BMC Ecol. 11, 13. <https://doi.org/10.1186/1472-6785-11-13>
- 605 Huson, D.H., Bryant, D., 2006. Application of phylogenetic networks in evolutionary studies. Mol.  
606 Biol. Evol. 23, 254–267. <https://doi.org/10.1093/molbev/msj030>

- 607 Insuan, S., Deowanish, S., Klinbunga, S., Sittipraneed, S., Sylvester, H.A., Wongsiri, S., 2007.  
608 Genetic Differentiation of the Giant Honey Bee (*Apis dorsata*) in Thailand Analyzed by  
609 Mitochondrial Genes and Microsatellites. *Biochem. Genet.* 45, 345–361.  
610 <https://doi.org/10.1007/s10528-007-9079-9>
- 611 Karanth, K.P., Singh, L., Collura, R. V., Stewart, C.B., 2008. Molecular phylogeny and  
612 biogeography of langurs and leaf monkeys of South Asia (Primates: Colobinae). *Mol.*  
613 *Phylogenet. Evol.* 46, 683–694. <https://doi.org/10.1016/j.ympev.2007.11.026>
- 614 Khonsanit, A., Luangsa-ard, J.J., Thanakitpipattana, D., Kobmoo, N., Piasai, O., 2019. Cryptic  
615 species within *Ophiocordyceps myrmecophila* complex on formicine ants from Thailand.  
616 *Mycol. Prog.* <https://doi.org/10.1007/s11557-018-1412-7>
- 617 Kishino, H., Hasegawa, M., 1989. Evaluation of the maximum likelihood estimate of the  
618 evolutionary tree topologies from DNA sequence data, and the branching order in hominoidea.  
619 *J. Mol. Evol.* 29, 170–179. <https://doi.org/10.1007/BF02100115>
- 620 Kobmoo, N., Mongkolsamrit, S., Tasanathai, K., Thanakitpipattana, D., Luangsa-Ard, J.J., 2012.  
621 Molecular phylogenies reveal host-specific divergence of *Ophiocordyceps unilateralis* sensu  
622 lato following its host ants. *Mol. Ecol.* 21, 3022–3031. <https://doi.org/10.1111/j.1365-294X.2012.05574.x>
- 624 Kobmoo, N., Mongkolsamrit, S., Wutikhun, T., Tasanathai, K., Khonsanit, A., Thanakitpipattana,  
625 D., Luangsa-Ard, J.J., 2015. New species of *Ophiocordyceps unilateralis*, an ubiquitous  
626 pathogen of ants from Thailand. *Fungal Biol.* 119, 44–52.  
627 <https://doi.org/10.1016/j.funbio.2014.10.008>
- 628 Kobmoo, N., Wichadakul, D., Arnarnart, N., Rodríguez De La Vega, R.C., Luangsa-ard, J.J.,  
629 Giraud, T., 2018. A genome scan of diversifying selection in *Ophiocordyceps* zombie-ant fungi  
630 suggests a role for enterotoxins in co-evolution and host specificity. *Mol. Ecol.* 27, 3582–3598.  
631 <https://doi.org/10.1111/mec.14813>
- 632 Kurtz, S., Phillippy, A., Delcher, A.L., Smoot, M., Shumway, M., Antonescu, C., Salzberg, S.L.,  
633 2004. Versatile and open software for comparing large genomes. *Genome Biol.* 5, R12. <https://doi.org/10.1186/gb-2004-5-2-r12>
- 635 Laciny, A., Druzhinina, I.S., Lim, L., Kopchinskiy, A., Zettel, H., Abu Salim, K., Pal, A.,  
636 Hoenigsberger, M., Javad Rahimi, M., Jaitrong, W., Pretzer, C., 2018. *Colobopsis explodens*  
637 sp. n., model species for studies on “exploding ants” (Hymenoptera, Formicidae), with  
638 biological notes and first illustrations of males of the *Colobopsis cylindrica* group. *Zookeys*  
639 751, 1–40. <https://doi.org/10.3897/zookeys.751.22661>
- 640 Larget, B.R., Kotha, S.K., Dewey, C.N., Ané, C., 2010. BUCKy: Gene tree/species tree  
641 reconciliation with Bayesian concordance analysis *Bret. Bioinformatics* 26, 2910–2911.  
642 <https://doi.org/10.1007/s00285-010-0355-7>
- 643 Li, H., 2013. Aligning sequence reads, clone sequences and assembly contigs with BWA-MEM.  
644 ArXiv: 1303.3997v2 [q-bio.GN]. <https://doi.org/10.1186/s13756-018-0352-y>

- 645 Lifjeld, J.T., 2015. When taxonomy meets genomics: lessons from a common songbird. *Mol. Ecol.*  
646 2901–2903. <https://doi.org/10.14344/IOC.ML.5.2>
- 647 Loreto, R.G., Elliot, S.L., Freitas, M.L.R., Pereira, T.M., Hughes, D.P., 2014. Long-term disease  
648 dynamics for a specialized parasite of ant societies: A field study. *PLoS One* 9, e103516.  
649 <https://doi.org/10.1371/journal.pone.0103516>
- 650 Luangsa-ard, J.J., Ridkaew, R., Tسانathai, K., Thanakitpipattana, D., Hywel-Jones, N., 2011.  
651 *Ophiocordyceps halabalaensis*: A new species of *Ophiocordyceps* pathogenic to *Camponotus*  
652 *gigas* in Hala Bala Wildlife Sanctuary, Southern Thailand. *Fungal Biol.* 115, 608–614.  
653 <https://doi.org/10.1016/j.funbio.2011.03.002>
- 654 Matute, D.R., Sepúlveda, V.E., 2019. Fungal species boundaries in the genomics era. *Fungal Genet.*  
655 *Biol.* 103249. <https://doi.org/10.1016/j.fgb.2019.103249>
- 656 McKenna, A., Hanna, M., Banks, E., Sivachenko, A., Cibulskis, K., Kernytsky, A., Garimella, K.,  
657 Altshuler, D., Gabriel, S., Daly, M., DePristo, M.A., 2010. The Genome Analysis Toolkit: a  
658 MapReduce framework for analyzing next-generation DNA sequencing data. *Genome Res.* 20,  
659 1297–1303. <https://doi.org/10.1101/gr.107524.110>
- 660 Miraldo, A., Li, S., Borregaard, M.K., Flórez-Rodríguez, A., Gopalakrishnan, S., Rizvanovic, M.,  
661 Wang, Z., Rahbek, C., Marske, K.A., Nogués-Bravo, D., 2016. An Anthropocene map of  
662 genetic diversity. *Science.* 353, 1532–1535. <https://doi.org/10.1126/science.aaf4381>
- 663 Molina, M.C., Del-Prado, R., Divakar, P.K., Sánchez-Mata, D., Crespo, A., 2011. Another example  
664 of cryptic diversity in lichen-forming fungi: The new species *Parmelia mayi* (Ascomycota:  
665 Parmeliaceae). *Org. Divers. Evol.* 11, 331–342. <https://doi.org/10.1007/s13127-011-0060-4>
- 666 Mongkolsamrit, S., Kobmoo, N., Tسانathai, K., Khonsanit, A., Noisriboom, W., Srikitikulchai, P.,  
667 Somnuk, R., Luangsa-ard, J.J., 2012. Life cycle, host range and temporal variation of  
668 *Ophiocordyceps unilateralis/Hirsutella formicarum* on Formicine ants. *J. Invertebr. Pathol.*  
669 111. <https://doi.org/10.1016/j.jip.2012.08.007>
- 670 Mongkolsamrit, S., Noisriboom, W., Thanakitpipattana, D., Wutikhun, T., Spatafora, J.W., Luangsa-  
671 ard, J., 2018. Disentangling cryptic species with isaria-like morphs in Cordycipitaceae.  
672 *Mycologia.* 110, 230–257. <https://doi.org/10.1080/00275514.2018.1446651>
- 673 Montarry, J., Cartolaro, P., Richard-Cervera, S., Delmotte, F., 2009. Spatio-temporal distribution of  
674 *Erysiphe necator* genetic groups and their relationship with disease levels in vineyards. *Eur. J.*  
675 *Plant Pathol.* <https://doi.org/10.1007/s10658-008-9343-9>
- 676 Morand, S., Krasnov, B.R., Littlewood, T.J. (Eds.), 2015. Parasite Diversity and Diversification:  
677 Evolutionary Ecology Meets Phylogenetics. Cambridge University Press.  
678 <https://doi.org/10.1017/CBO9781139794749>
- 679 Nieuwenhuis, B.P.S., James, T.Y., 2016. The frequency of sex in fungi. *Philos. Trans. R. Soc. B*  
680 *Biol. Sci.* 371, 20150540. <https://doi.org/10.1098/rstb.2015.0540>

681 Pfeifer, B., Wittelsbürger, U., Ramos-Onsins, S.E., Lercher, M.J., 2014. PopGenome: An efficient  
682 swiss army knife for population genomic analyses in R. Mol. Biol. Evol.  
683 <https://doi.org/10.1093/molbev/msu136>

684 Pickrell, J.K., Pritchard, J.K., 2012. Inference of Population Splits and Mixtures from Genome-  
685 Wide Allele Frequency Data. PLoS Genet. 8, e1002967.  
686 <https://doi.org/10.1371/journal.pgen.1002967>

687 Pramual, P., Kuvangkadilok, C., Baimai, V., Walton, C., 2005. Phylogeography of the black fly  
688 *Simulium tani* (Diptera: Simuliidae) from Thailand as inferred from mtDNA sequences. Mol.  
689 Ecol. 14, 3989–4001. <https://doi.org/10.1111/j.1365-294X.2005.02639.x>

690 Purcell, S., Neale, B., Todd-Brown, K., Thomas, L., Ferreira, M.A.R., Bender, D., Maller, J., Sklar,  
691 P., de Bakker, P.I.W., Daly, M.J., Sham, P.C., 2007. PLINK: a tool set for whole-genome  
692 association and population-based linkage analyses. Am. J. Hum. Genet. 81, 559–575.  
693 <https://doi.org/10.1086/519795>

694 Raj, A., Stephens, M., Pritchard, J.K., 2014. fastSTRUCTURE: Variational Inference of Population  
695 Structure in Large SNP Data Sets. Genetics 197, 573–589.  
696 <https://doi.org/10.1534/genetics.114.164350>

697 Ronquist, F., Teslenko, M., van der Mark, P., Ayres, D.L., Darling, A., Höhna, S., Larget, B., Liu,  
698 L., Suchard, M.A., Huelsenbeck, J.P., 2012. MrBayes 3.2: Efficient Bayesian Phylogenetic  
699 Inference and Model Choice Across a Large Model Space. Syst. Biol. 61, 539–542.  
700 <https://doi.org/10.1093/sysbio/sys029>

701 Rousset, F., 1997. Genetic Differentiation and Estimation of Gene Flow from F-Statistics Under  
702 Isolation by Distance. Genetics 145, 1219–1228.

703 Savary, R., Masclaux, F.G., Wyss, T., Droh, G., Cruz Corella, J., Machado, A.P., Morton, J.B.,  
704 Sanders, I.R., 2018. A population genomics approach shows widespread geographical  
705 distribution of cryptic genomic forms of the symbiotic fungus *Rhizophagus irregularis*. ISME  
706 J. 12, 17–30. <https://doi.org/10.1038/ismej.2017.153>

707 Scrucca, L., Fop, M., Murphy, T.B., Raftery, A.E., 2016. mclust 5: Clustering, Classification and  
708 Density Estimation Using Gaussian Finite Mixture Models. R J. 8, 289–317.  
709 <https://doi.org/10.1177/2167702614534210>

710 Sepúlveda, V.E., Marquez, R., Turissini, D.A., Goldman, W.E., Matute, D.R., 2017. Genome  
711 Sequences Reveal Cryptic Speciation in the Human Pathogen *Histoplasma capsulatum*. mBio  
712 8, e01339-17.

713 Sittipraneed, S., Sihanuntavong, D., Klinbunga, S., 2001. Genetic differentiation of the honey bee  
714 (*Apis cerana*) in Thailand revealed by polymorphism of a large subunit of mitochondrial  
715 ribosomal DNA. Insectes Sociaux. 48, 266–272. <https://doi.org/10.1007/PL00001776>

716 Smit, A.F.A., Hubley, R., Green, P., n.d. RepeatMasker Open-4.0. [WWW Document]. URL [http://](http://www.repeatmasker.org)  
717 [www.repeatmasker.org](http://www.repeatmasker.org)

- 718 Smith, B.T., Seeholzer, G.F., Harvey, M.G., Cuervo, A.M., Brumfield, R.T., 2017. A latitudinal  
719 phylogeographic diversity gradient in birds. *PLoS Biol.* 15, 1–24.  
720 <https://doi.org/10.1371/journal.pbio.2001073>
- 721 Struck, T.H., Feder, J.L., Bendiksby, M., Birkeland, S., Cerca, J., Gusarov, V.I., Kistenich, S.,  
722 Larsson, K.H., Liow, L.H., Nowak, M.D., Stedje, B., Bachmann, L., Dimitrov, D., 2018.  
723 Finding Evolutionary Processes Hidden in Cryptic Species. *Trends Ecol. Evol.* 33, 153–163.  
724 <https://doi.org/10.1016/j.tree.2017.11.007>
- 725 Stukenbrock, E.H., Dutheil, J.Y., 2018. Fine-Scale Recombination Maps of Fungal Plant 208, 1209–  
726 1229. <https://doi.org/10.1534/genetics.117.300502/-/DC1.1>
- 727 Taylor, J.W., Hann-Soden, C., Branco, S., Sylvain, I., Ellison, C.E., 2015. Clonal reproduction in  
728 fungi. *Proc. Natl. Acad. Sci.* 112, 8901–8908. <https://doi.org/10.1073/pnas.1503159112>
- 729 Taylor, J.W., Jacobson, D.J., Kroken, S., Kasuga, T., Geiser, D.M., Hibbett, D.S., Fisher, M.C.,  
730 2000. Phylogenetic Species Recognition and Species Concepts in Fungi. *Fungal Genet. Biol.*  
731 31, 21–32. <https://doi.org/10.1006/fgbi.2000.1228>
- 732 Tsai, I.J., Bensasson, D., Burt, A., Koufopanou, V., 2008. Population genomics of the wild yeast  
733 *Saccharomyces paradoxus*: Quantifying the life cycle. *Proc. Natl. Acad. Sci.* 105, 4957–4962.  
734 <https://doi.org/10.1073/pnas.0707314105>
- 735 Tu, V.T., Csorba, G., Ruedi, M., Furey, N.M., Son, N.T., Thong, V.D., Bonillo, C., Hassanin, A.,  
736 2017. Comparative phylogeography of bamboo bats of the genus *Tylonycteris* (Chiroptera,  
737 Vespertilionidae) in Southeast Asia. *Eur. J. Taxon.* 1–38. <https://doi.org/10.5852/ejt.2017.274>
- 738 Vercken, E., Fontaine, M.C., Gladieux, P., Hood, M.E., Jonot, O., Giraud, T., 2010. Glacial refugia  
739 in pathogens: European genetic structure of anther smut pathogens on *Silene latifolia* and  
740 *Silene dioica*. *PLoS Pathog.* 6, e1001229. <https://doi.org/10.1371/journal.ppat.1001229>
- 741 Vincenot, L., Popa, F., Laso, F., Donges, K., Rexer, K.H., Kost, G., Yang, Z.L., Nara, K., Selosse,  
742 M.A., 2017. Out of Asia: Biogeography of fungal populations reveals Asian origin of  
743 diversification of the *Laccaria amethystina* complex, and two new species of violet *Laccaria*.  
744 *Fungal Biol.* 121, 939–955. <https://doi.org/10.1016/j.funbio.2017.08.001>
- 745 Ward, P.S., Blaimer, B.B., Fisher, B.L., 2016. A revised phylogenetic classification of the ant  
746 subfamily Formicinae (Hymenoptera: Formicidae), with resurrection of the genera *Colobopsis*  
747 and *Dinomyrmex*. *Zootaxa* 4072, 343–357. <https://doi.org/10.11646/zootaxa.4072.3.4>
- 748 Weiss, M., Weigand, H., Weigand, A.M., Leese, F., 2018. Genome-wide single-nucleotide  
749 polymorphism data reveal cryptic species within cryptic freshwater snail species—The case of  
750 the *Ancylus fluviatilis* species complex. *Ecol. Evol.* 8, 1063–1072.  
751 <https://doi.org/10.1002/ece3.3706>
- 752 Woodruff, D.S., 2010. Biogeography and conservation in Southeast Asia: How 2.7 million years of  
753 repeated environmental fluctuations affect today’s patterns and the future of the remaining

754 refugial-phase biodiversity. *Biodivers. Conserv.* 19, 919–941. [https://doi.org/10.1007/s10531-](https://doi.org/10.1007/s10531-010-9783-3)  
755 [010-9783-3](https://doi.org/10.1007/s10531-010-9783-3)

756 Yu, H., Tian, E., Zheng, L., Deng, X., Cheng, Y., Chen, L., Wu, W., Tanming, W., Zhang, D.,  
757 Compton, S.G., Kjellberg, F., 2019. Multiple parapatric pollinators have radiated across a  
758 continental fig tree displaying clinal genetic variation. *Mol. Ecol.*  
759 <https://doi.org/10.1111/mec.15046>  
760

## 761 **Figures Captions**

762 **Figure 1.** a) Sampling sites of *Ophiocordyceps unilateralis sensu lato* across Thailand (1 = Ban  
763 Huai Baba, 2 = Doi Inthanon National Park, 3 = Nam Nao National Park, 4 = Phu Khiao Wildlife  
764 Sanctuary, 5 = Khao Yai National Park, 6 = Ko Chang Island, 7 = Khlong Nakha Wildlife  
765 Sanctuary, 8 = Khao Luang National Park, 9 = Hala Bala Wildlife Sanctuary). The pie charts  
766 represent the proportions of fungal samples collected on different ant species (CL red = *Colobopsis*  
767 *leonardi*, CS green = *Colobopsis saundersi*, PF blue = *Polyrhachis furcata*). b) Principal component  
768 analysis (PCA) based on whole genome single nucleotide polymorphisms (SNPs); colors  
769 correspond to the host species as in Figure 1a. c) Bayesian clustering based on whole genome single  
770 nucleotide polymorphisms (SNPs) (K=5). Vertical bars represent individuals and the colors their  
771 assignment probabilities to five genetic clusters. The arrows indicate the samples NK122ss and  
772 NK604. Numbers below the barplots represent the sample sites as in Figure 1a.

773

774 **Figure 2.** Maximum likelihood-based tree inferred using a) the whole genome altered at the SNP  
775 positions, b) separate scaffolds. The colors at the tips represent the identities of ant hosts (red =  
776 *Colobopsis leonardi*, green = *C. saundersi*, blue = *Polyrhachis furcata*). Thick branches correspond  
777 to those leading to nodes with 100% bootstrap support.

778

779

780 **Figure 3.** Bayesian inference-based trees with genome-wide concordance factors and their  
781 confidence intervals, supporting monophyletic clades representing a) the three host-specific species

782 (OCL = *Ophiocordyceps camponoti-leonardi*, OCS = *O. camponoti-saundersi*, OPF = *O.*  
783 *polyrhachis-furcata*), and b) different genetic clusters as inferred from Bayesian clustering (OCL1  
784 and OCL2 = *O. camponoti-leonardi* clusters 1 and 2; OCS1, OCS2 and OCS3 = *O. camponoti-*  
785 *saundersi* clusters 1, 2 and 3; OPF1 and OPF2 = *O. polyrhachis-furcata* clusters 1 and 2).  
786 Concordance factors (CF) can range from 0 to 1 (absence of concordance to complete  
787 concordance). In the panel a (left), the subclades identified in the panel b (right) were collapsed to  
788 better show the support for OCS, OPF and OCL.

789

790 **Figure 4.** Barplots of Bayesian clustering using single nucleotide polymorphisms (SNPs) inferred  
791 using conspecific genome references, with the geographical location of samples assigned to the  
792 different clusters, for each of the three species at K = 3: a) *Ophiocordyceps camponoti-leonardi*, b)  
793 *O. camponoti-saundersi* and c) *O. polyrhachis-furcata*.

794

795 **Figure 5.** A neighbor-net phylogenetic network of *Ophiocordyceps unilateralis* (OCL = *O.*  
796 *camponoti-leonardi*, OCS = *O. camponoti-saundersi*, OPF = *O. polyrhachis-furcata*).

797

798 **Figure 6.** Clustering of *Ophiocordyceps unilateralis sensu lato*, based on Gower's distance, along  
799 the *O. polyrhachis-furcata* BCC54312 reference genome using 500 SNPs sliding windows (OCL =  
800 *O. camponoti-leonardi*, OCS = *O. camponoti-saundersi*, OPF = *O. polyrhachis-furcata*). The red  
801 asterisk (★) indicates the sample NK561 with a footprint of admixture between OCL1 and OCL2.  
802 The red arrows (↔) point to the samples NK151 and NK157 of OPF which have a clear signature  
803 of admixture.

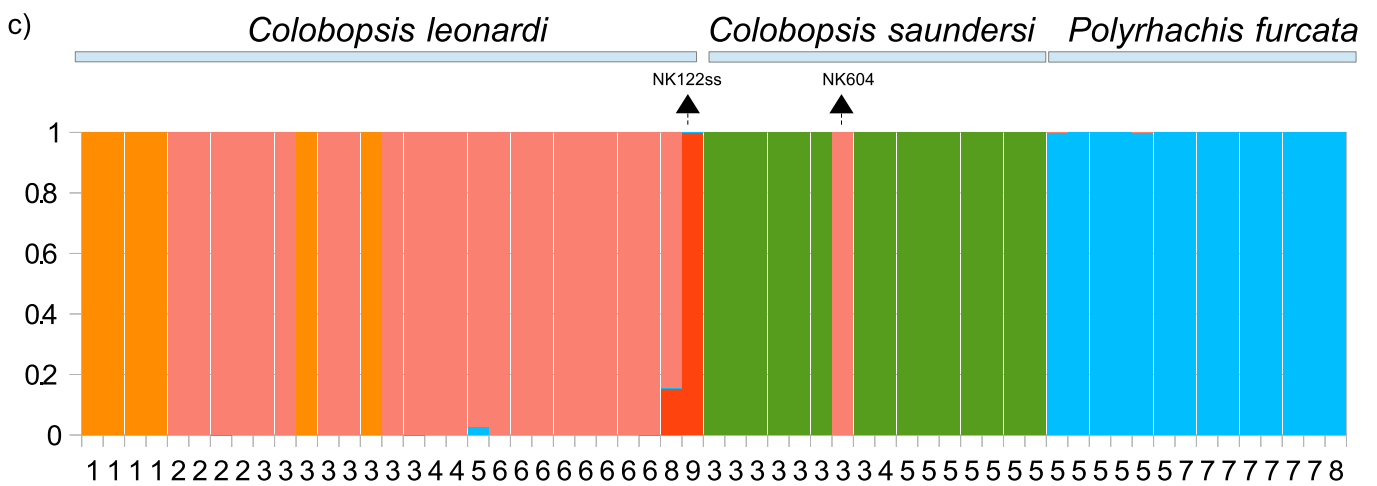
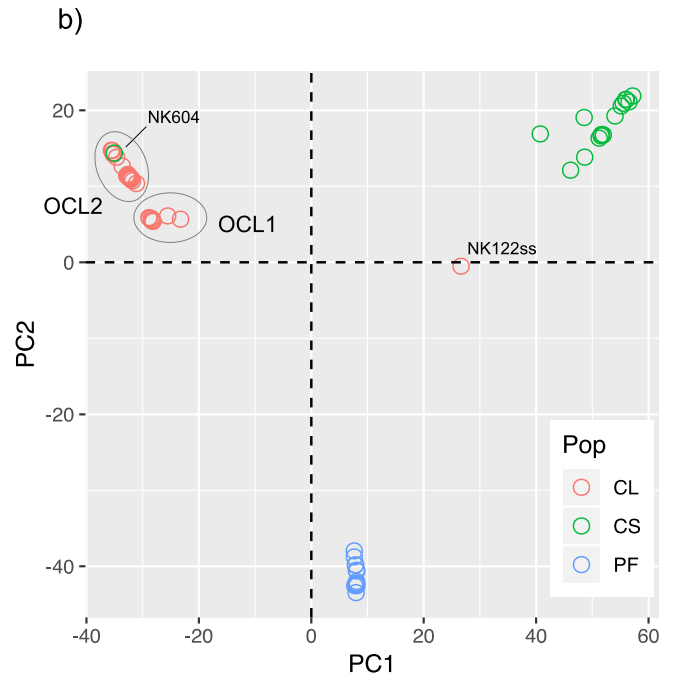
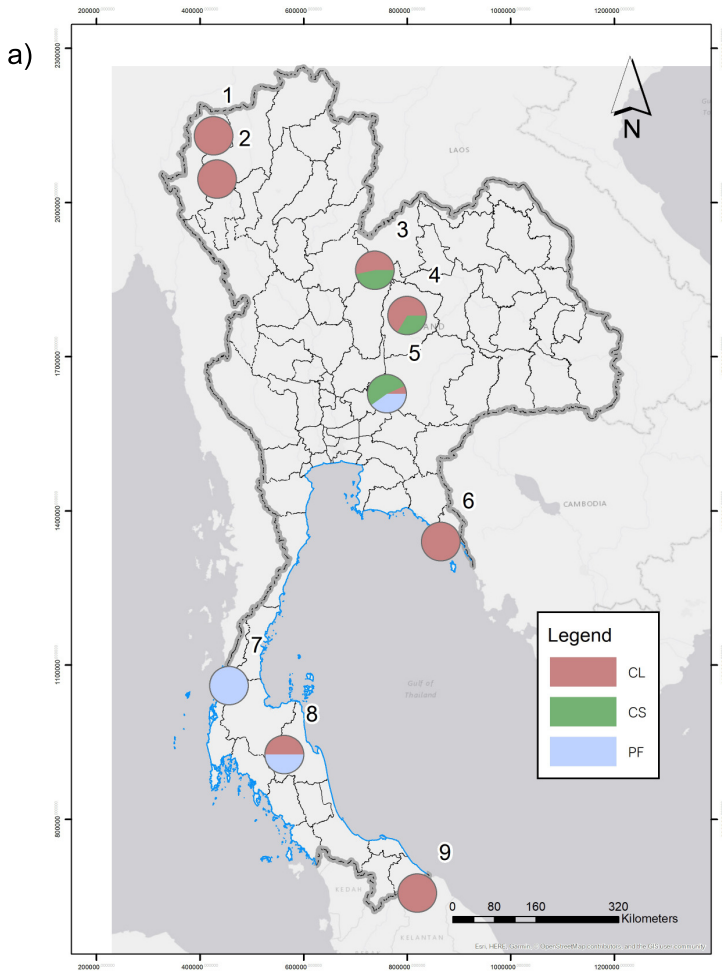
804

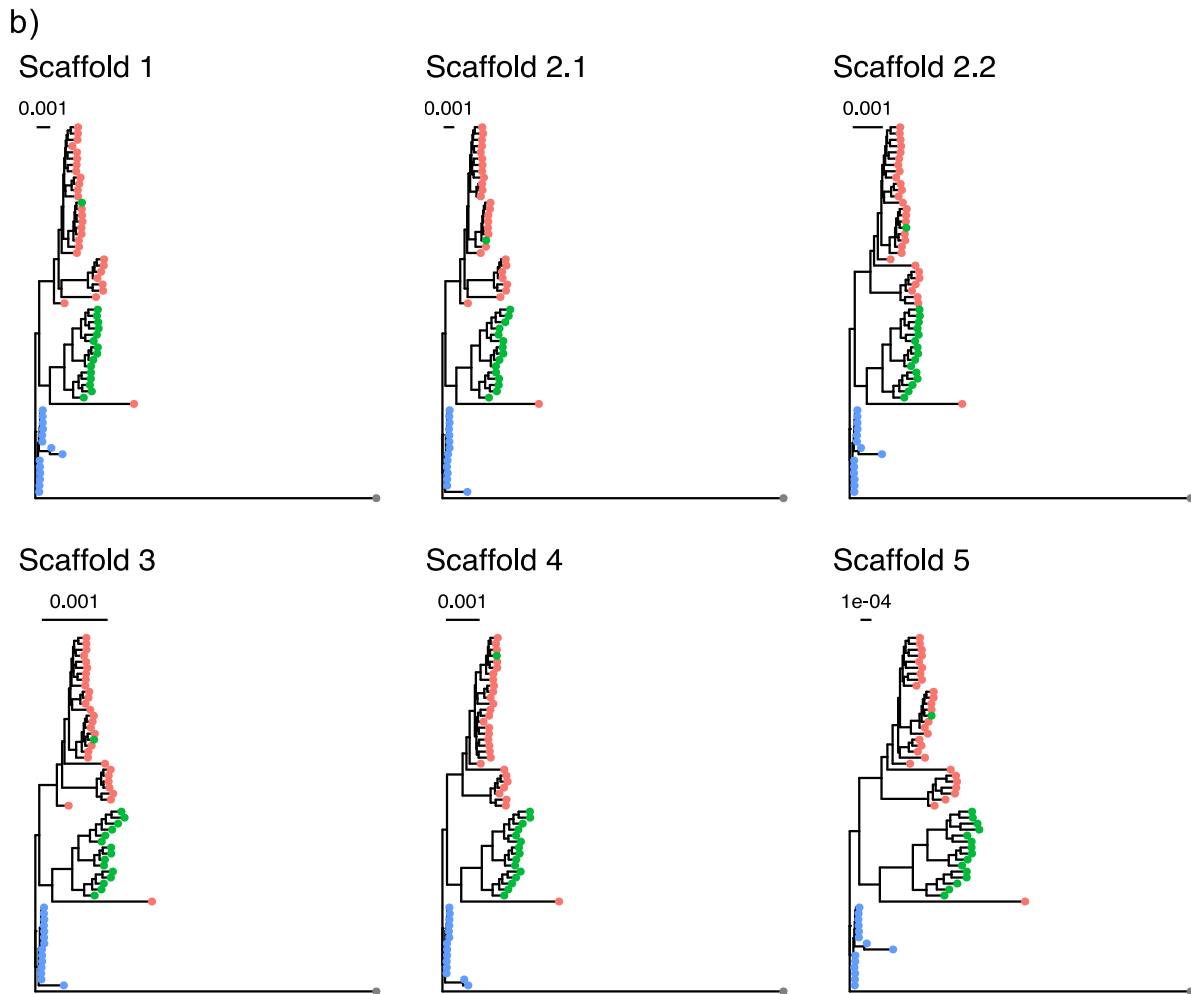
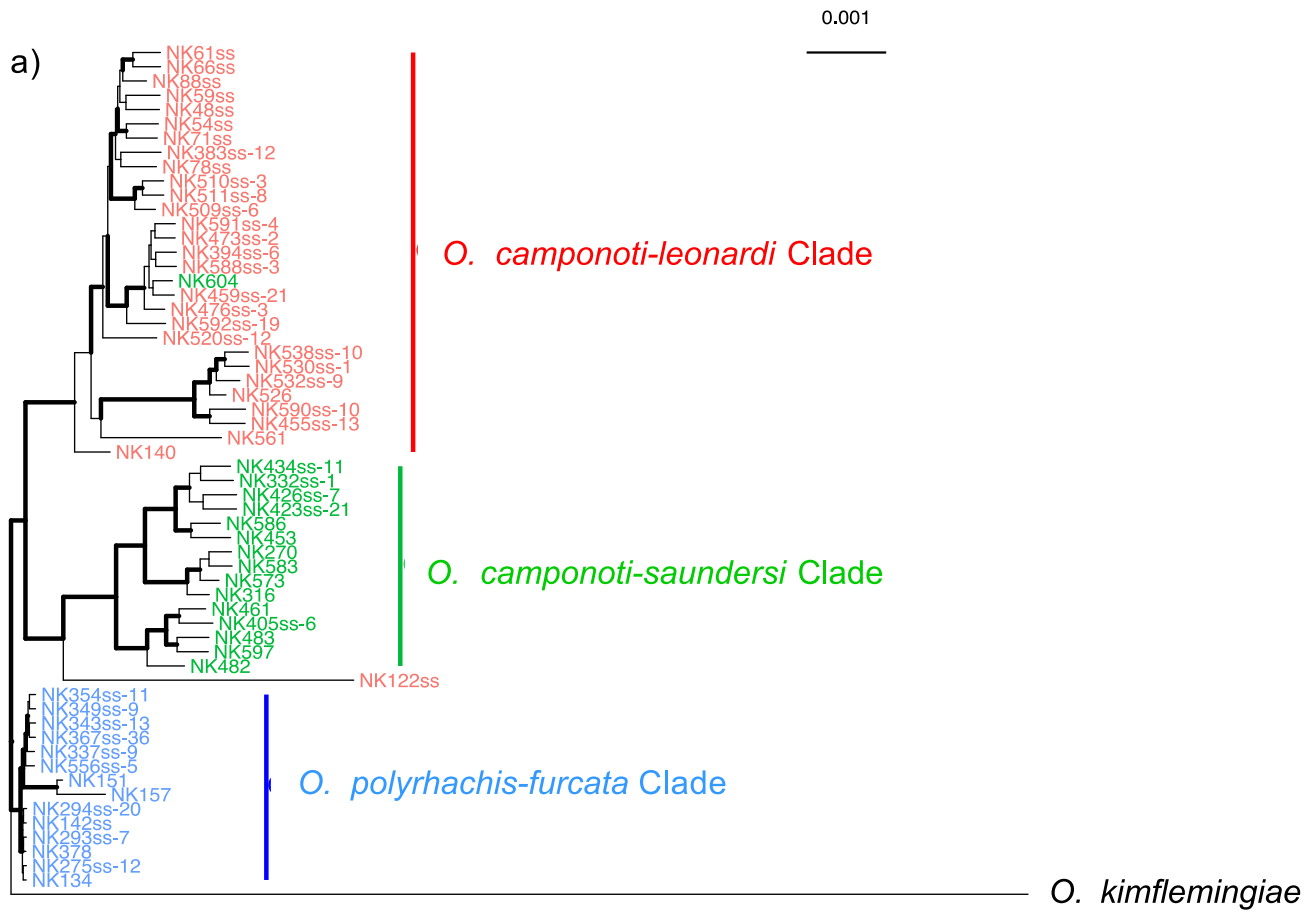
805 **Figure 7.** Results of TreeMix. a) Best-fitting genealogy without admixture (m=0) for different  
806 *Ophiocordyceps unilateralis* species and clusters as inferred from the variance-covariance matrix of

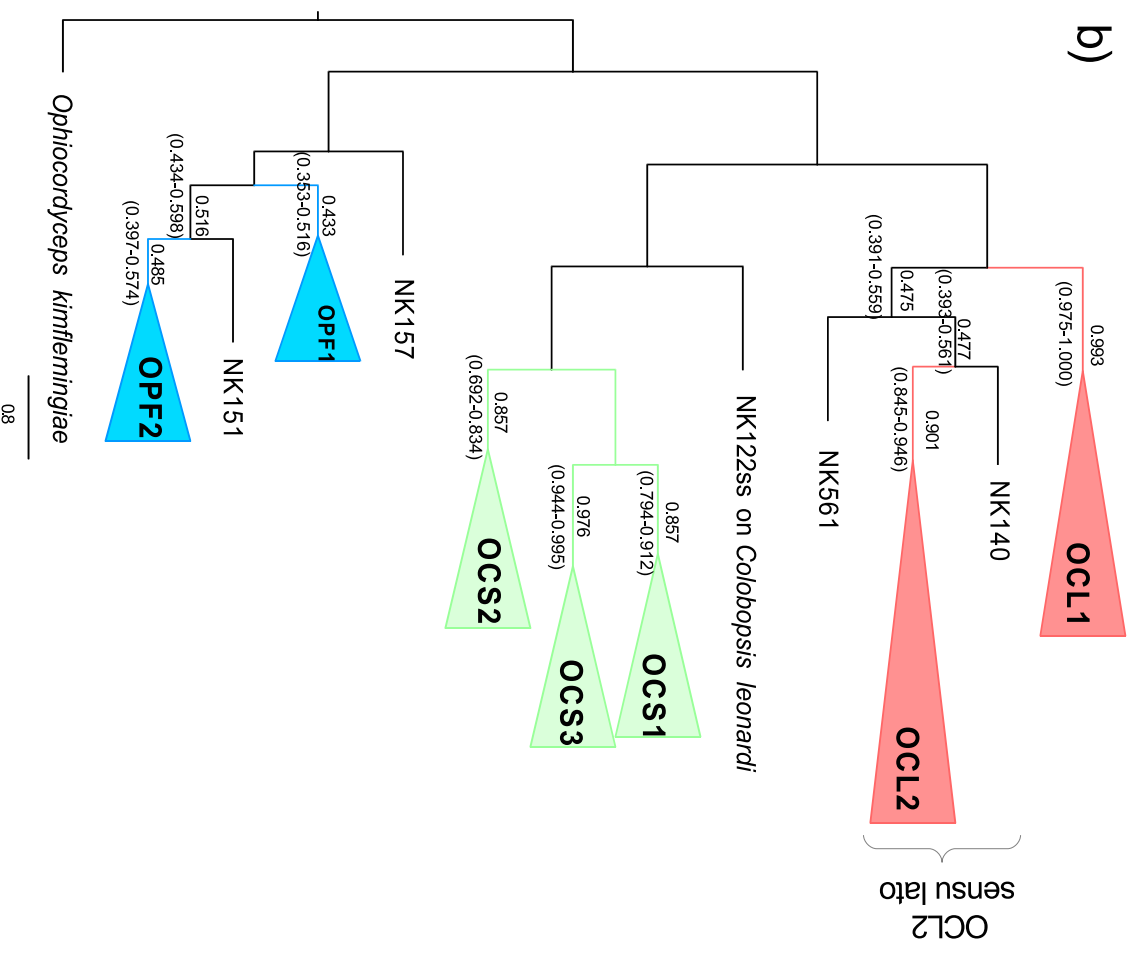
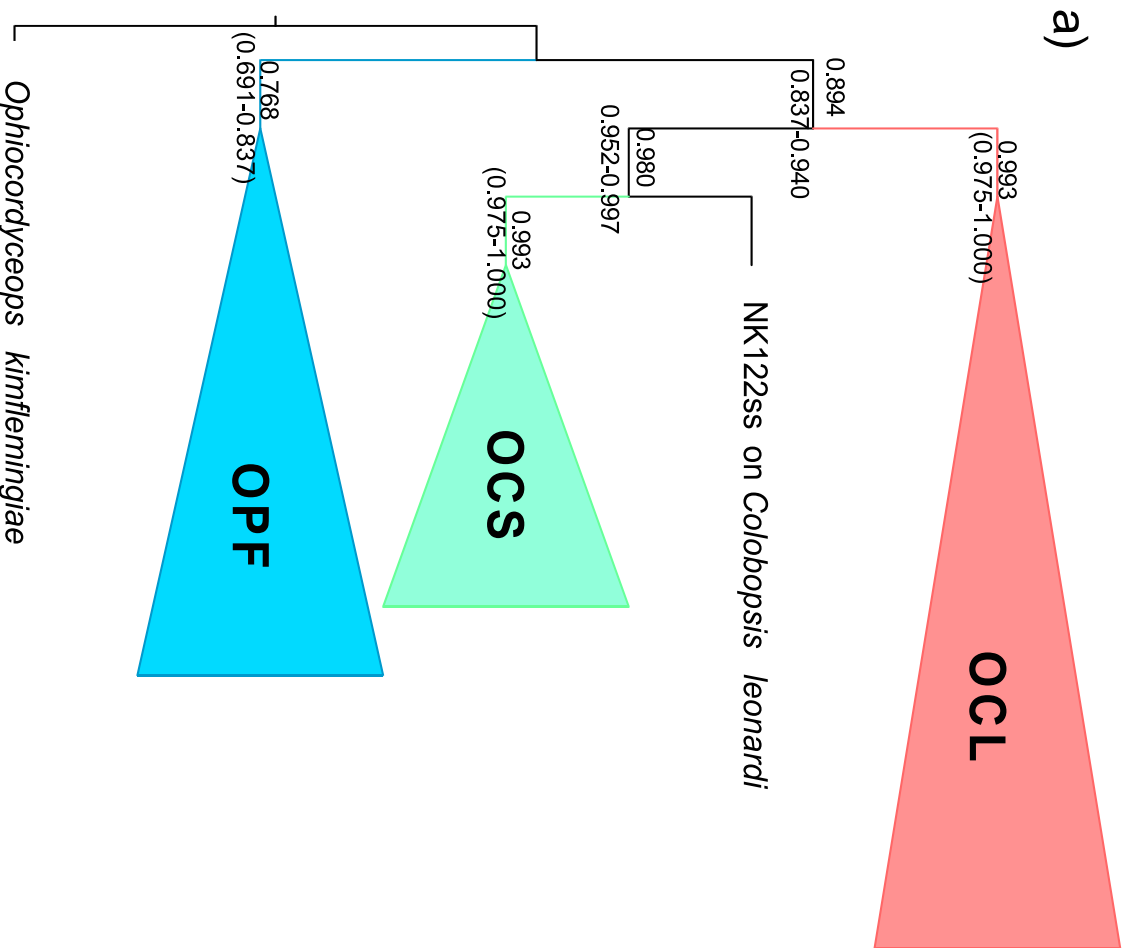
807 the genome-wide alleles frequencies based on the SNPs using *O. polyrhachis-furcata* as the  
808 reference. b) A scenario of one event of migration ( $m=1$ ). The model a) is nested within b). We  
809 estimated the likelihood of both scenarios and used a log likelihood ratio test (LRT) to determine  
810 the best-fitting scenario.

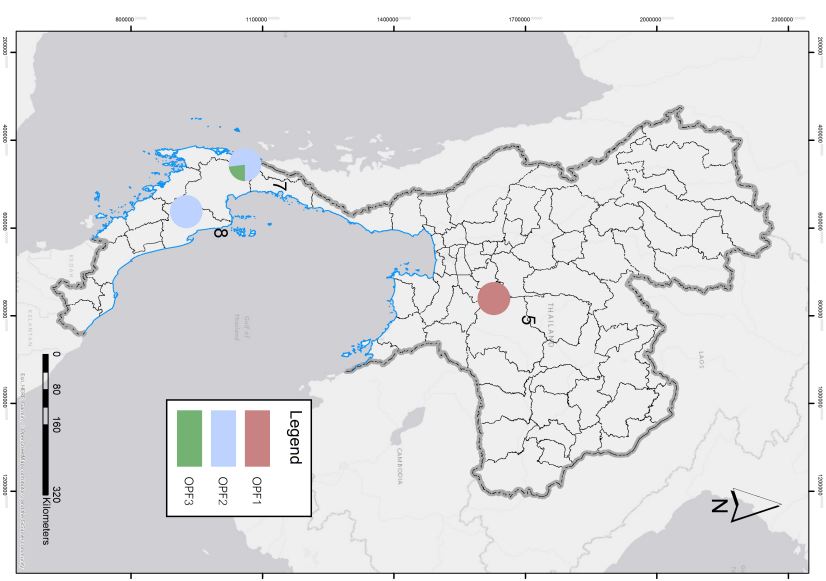
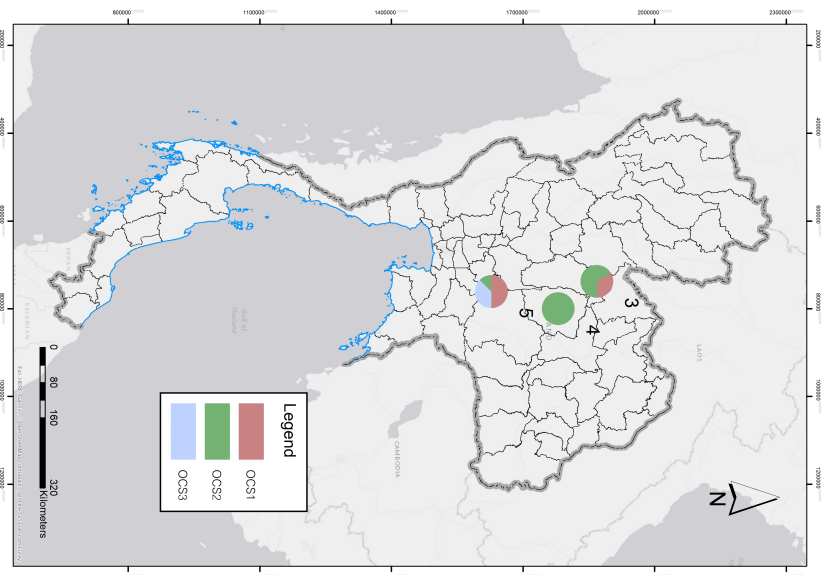
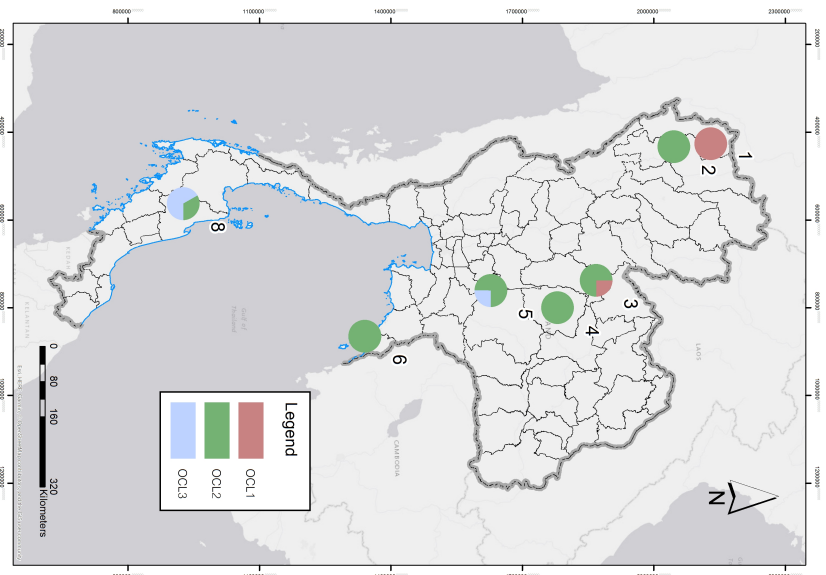
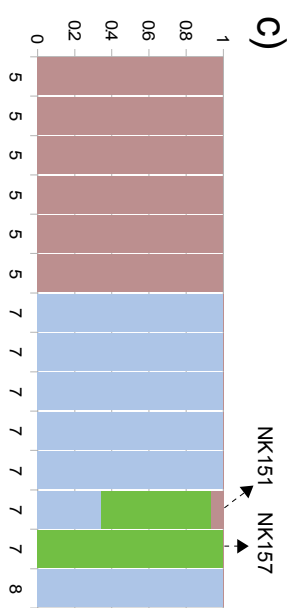
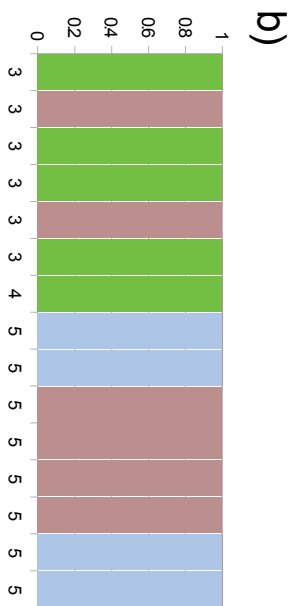
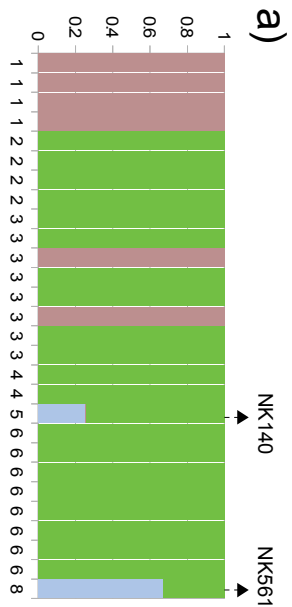
811

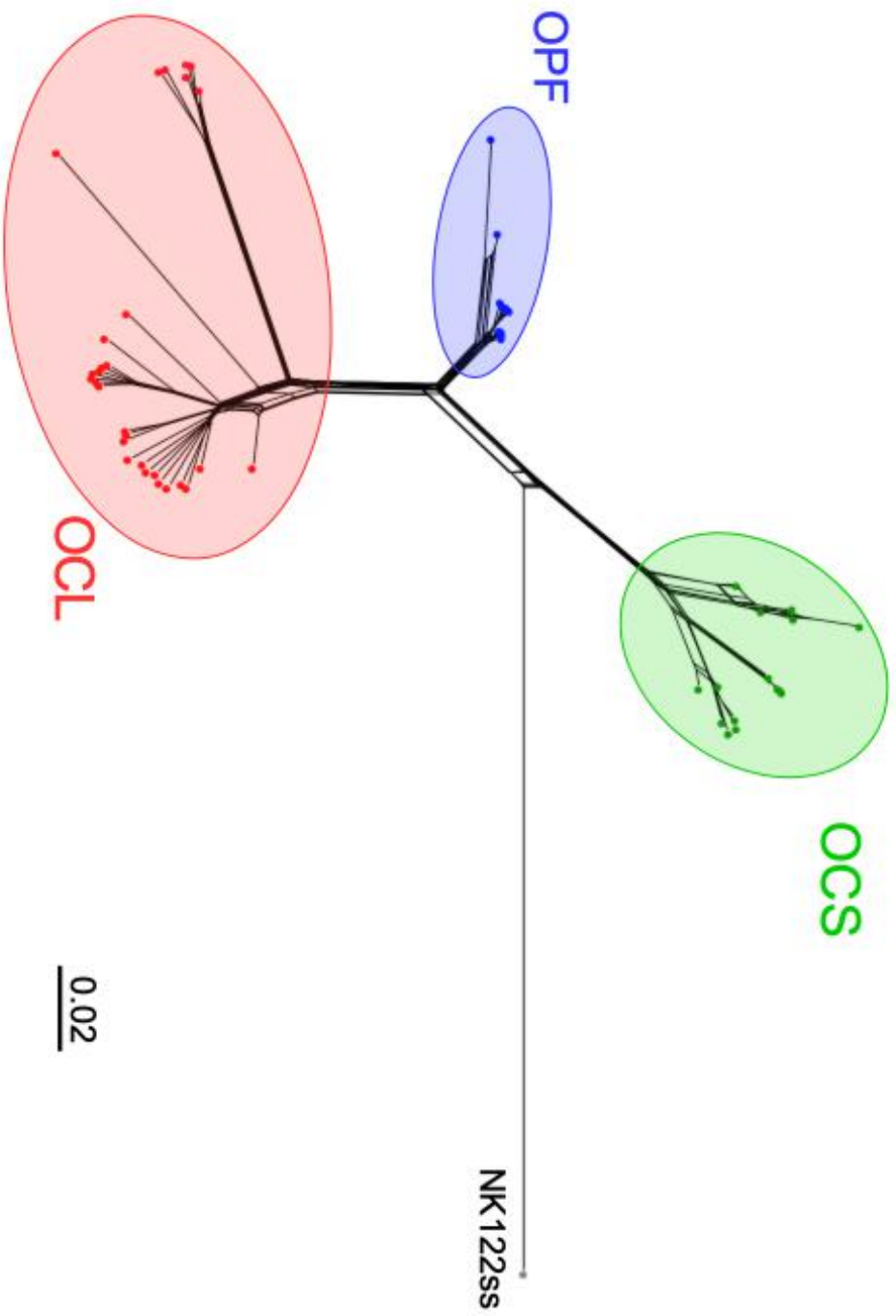
812 **Figure 8.** Linkage disequilibrium (LD) decay of *Ophiocordyceps camponoti-leonardi* (red), *O.*  
813 *camponoti-saundersi* (green) and *O. polyrhachis-furcata* (blue).

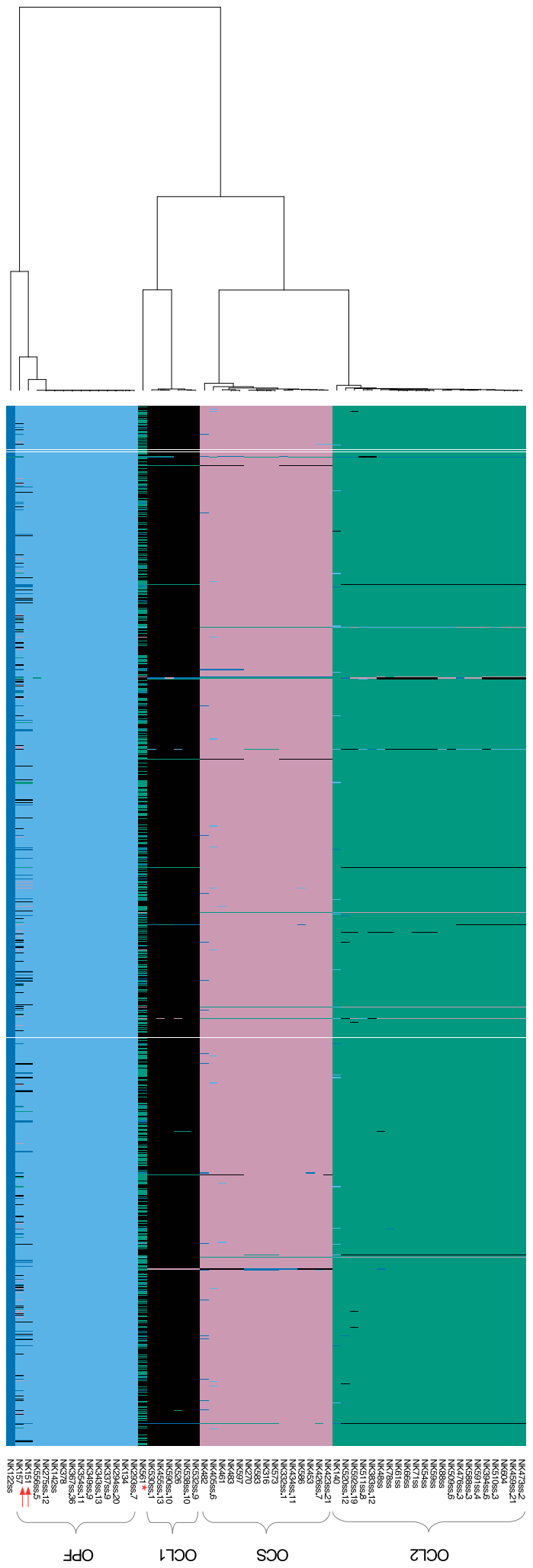
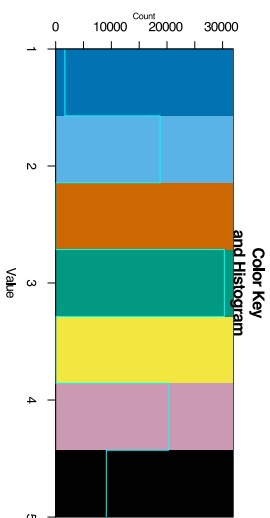




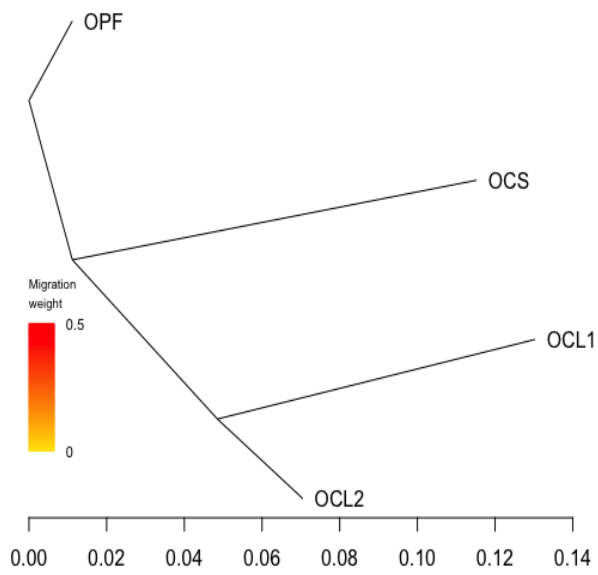




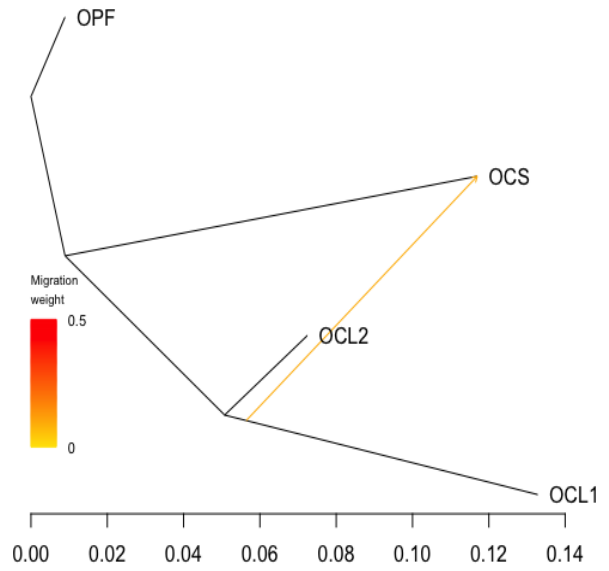


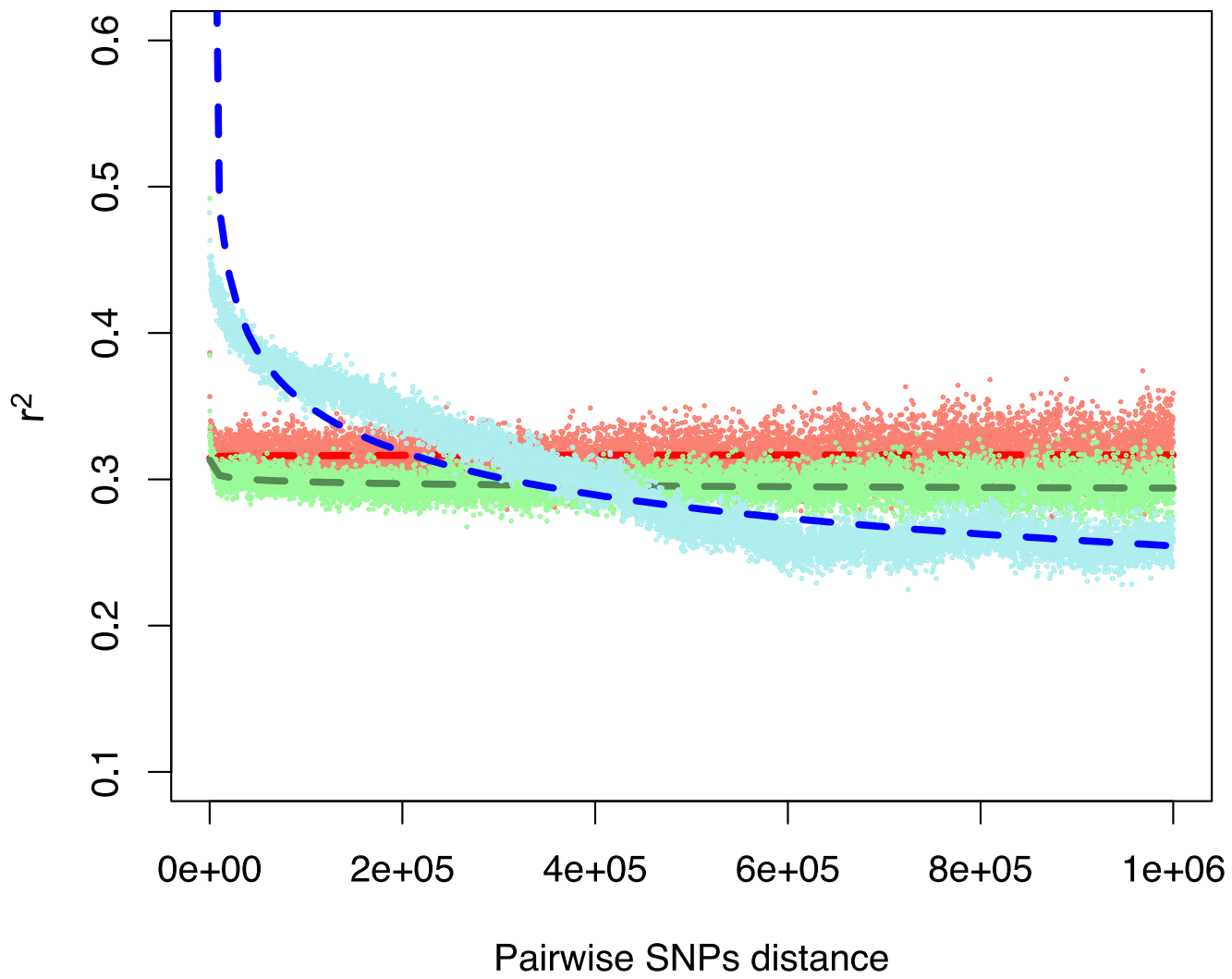


a.  $m=0$ ,  $\ln(\text{likelihood}) = 73.50$



b.  $m=1$ ,  $\ln(\text{likelihood}) = 74.95$ ,  $p\text{-value} = 0.2$





## Appendix A: Supplementary Figures

**Cryptic species within *Ophiocordyceps unilateralis* as revealed by population genomics**  
**The one ant-one fungus paradigm in *Ophiocordyceps unilateralis sensu lato* challenged by population genomics**

Noppol KOBMOO<sup>†‡</sup>, Suchada MONGKOLSAMRIT<sup>†</sup>, Nuntanat ARNAMNART<sup>†</sup>, Janet Jennifer LUANGSA-ARD<sup>†</sup>, Tatiana GIRAUD<sup>‡</sup>

<sup>†</sup> National Center for Genetic Engineering and Biotechnology (BIOTEC), National Science and Technology Development Agency (NSTDA), 113 Thailand Science Park, Phahonyothin Rd., Khlong Nueng, Khlong Luang, 12120 THAILAND.

<sup>‡</sup> Ecologie Systématique Evolution, Univ. Paris-Sud, CNRS, AgroParisTech, Université Paris-Saclay 91400 Orsay, France.

Corresponding author: Noppol Kobmoo,

E-mail: [noppol.kob@biotec.or.th](mailto:noppol.kob@biotec.or.th)

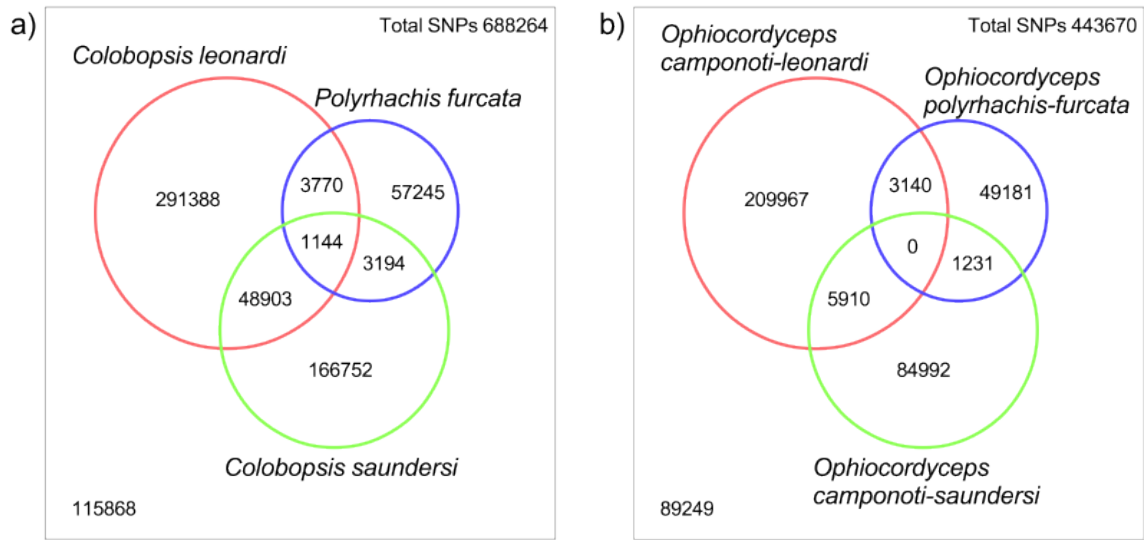
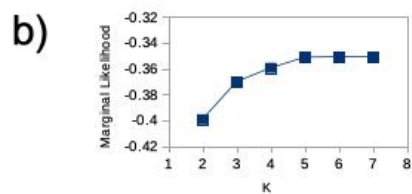
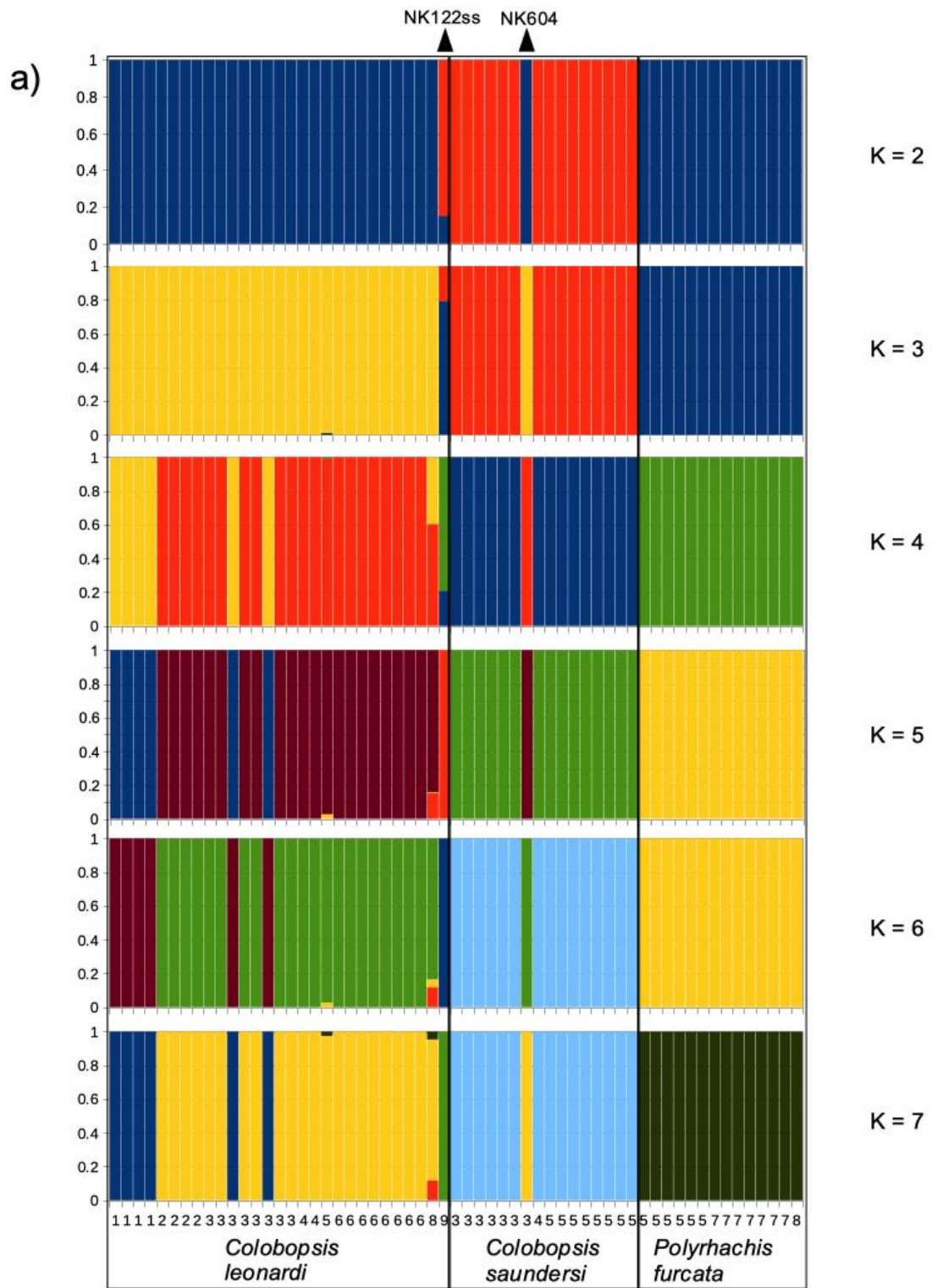


**Fig.S1** The number of single nucleotide polymorphisms (SNPs) shared between a) samples from different ant hosts, and b) samples of different fungal species.

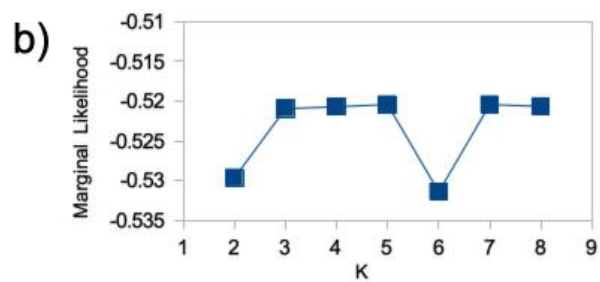
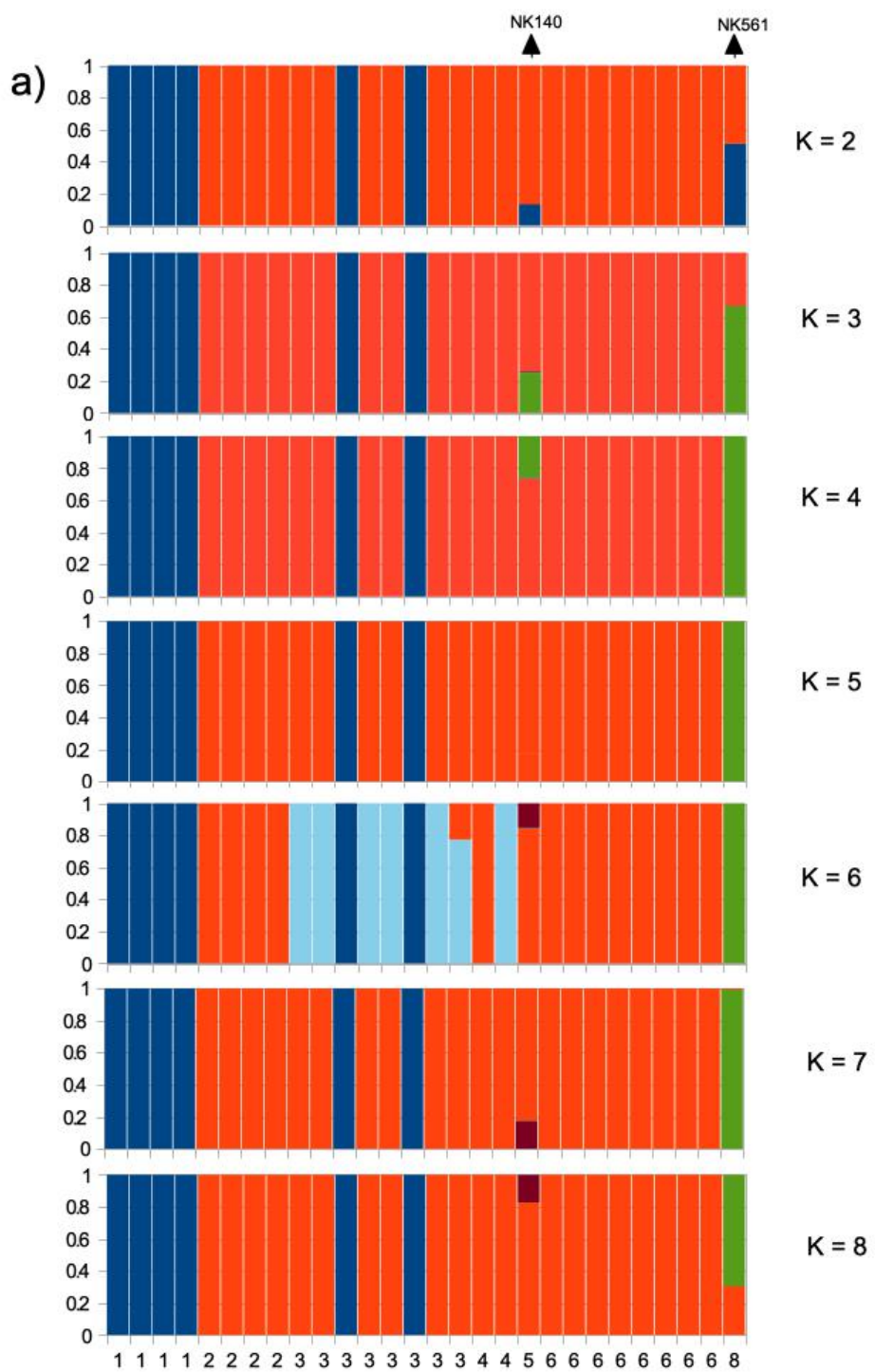
The figure S2 is given in a separate pdf file (FigS2.pdf) due to its big size.

**Fig.S2** Maximum likelihood-based trees inferred using separate scaffolds. The colors at the tips represent the identities of ant hosts (red = *Colobopsis leonardi*, green = *C. saundersi*, blue = *Polyrhachis furcata*). The black circles on nodes represent 100% bootstrap support.

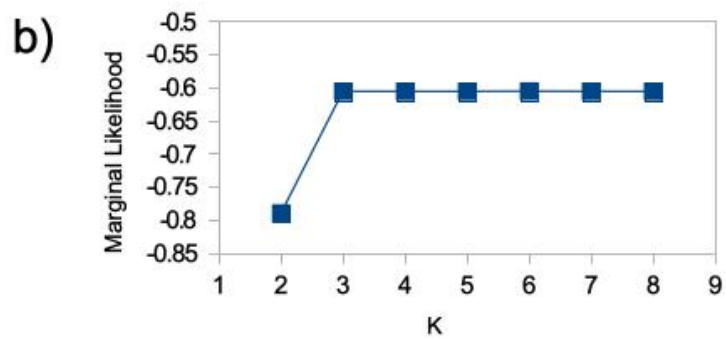
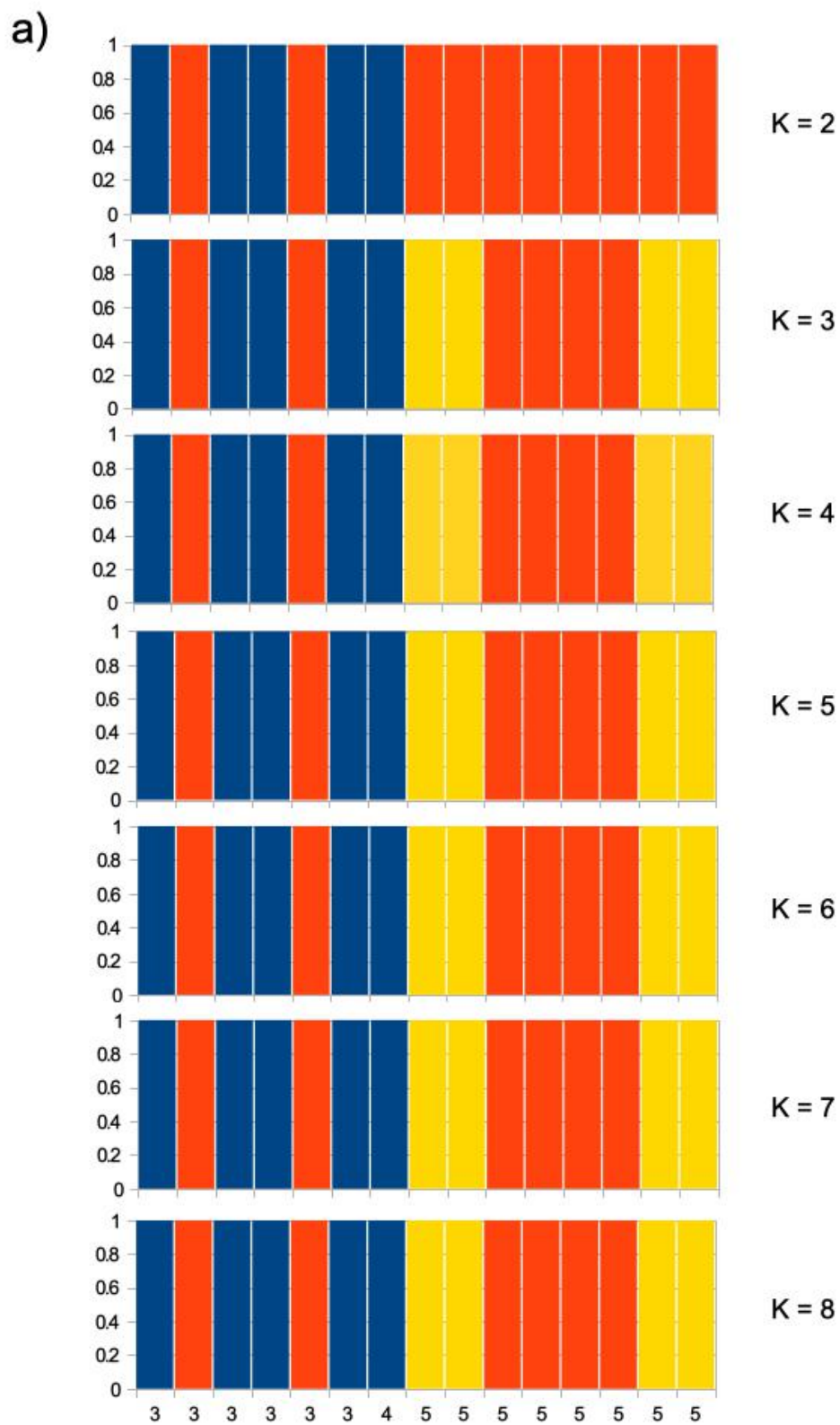
**Fig.S3** Bayesian clustering based on whole-genome single nucleotide polymorphisms (SNPs). a) Barplots of assignment probabilities to different clusters from K = 1 to K = 7. b) The marginal likelihood for different K values. 1 = Ban Huai Baba, 2 = Doi Inthanon National Park, 3 = Nam Nao National Park, 4 = Phu Khiao Wildlife Sanctuary, 5 = Khao Yai National Park, 6 = Ko Chang Island, 7 = Khlong Nakha Wildlife Sanctuary, 8 = Khao Luang National Park, 9 = Hala Bala Wildlife Sanctuary.



**Fig.S4** Bayesian clustering based on single nucleotide polymorphisms (SNPs) inferred from the reference genome of *Ophiocordyceps camponoti-leonardi* for the samples belonging to this species. a) Barplots of assignment probabilities to different clusters from  $K = 1$  to  $K = 8$  (The labels on the x axis correspond to the sampling sites). b) The marginal likelihood for different  $K$  values. 1 = Ban Huai Baba, 2 = Doi Inthanon National Park, 3 = Nam Nao National Park, 4 = Phu Khiao Wildlife Sanctuary, 5 = Khao Yai National Park, 6 = Ko Chang Island, 8 = Khao Luang National Park.



**Fig.S5** Bayesian clustering based on single nucleotide polymorphisms (SNPs) inferred from the reference genome of *Ophiocordyceps camponoti-saundersi* for the samples belonging to this species. a) Barplots of assignment probabilities to different clusters from  $K = 1$  to  $K = 8$  (The labels on the x axis correspond to the sampling sites). b) The marginal likelihood for different  $K$  values. 3 = Nam Nao National Park, 4 = Phu Khiao Wildlife Sanctuary, 5 = Khao Yai National Park.



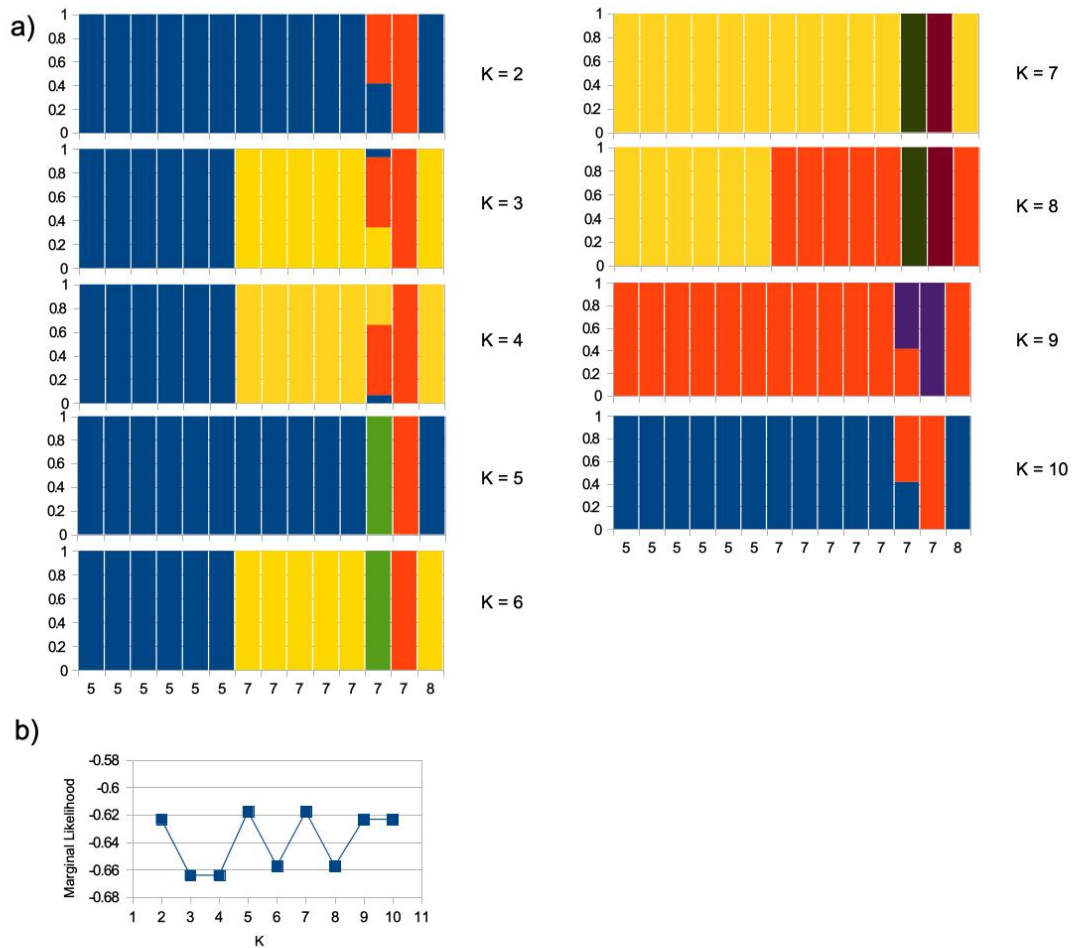


**Fig.S6** Bayesian clustering based on single nucleotide polymorphisms (SNPs) inferred from the reference genome of *Ophiocordyceps polyrhachis-furcata* for the samples belonging to this species. a) Barplots of assignment probabilities to different clusters from K = 1 to K = 8 (The labels on the x axis correspond to the sampling sites). b) The marginal likelihood for different K values. 5 = Khao Yai National Park, 7 = Khlong Nakha Wildlife Sanctuary, 8 = Khao Luang National Park.

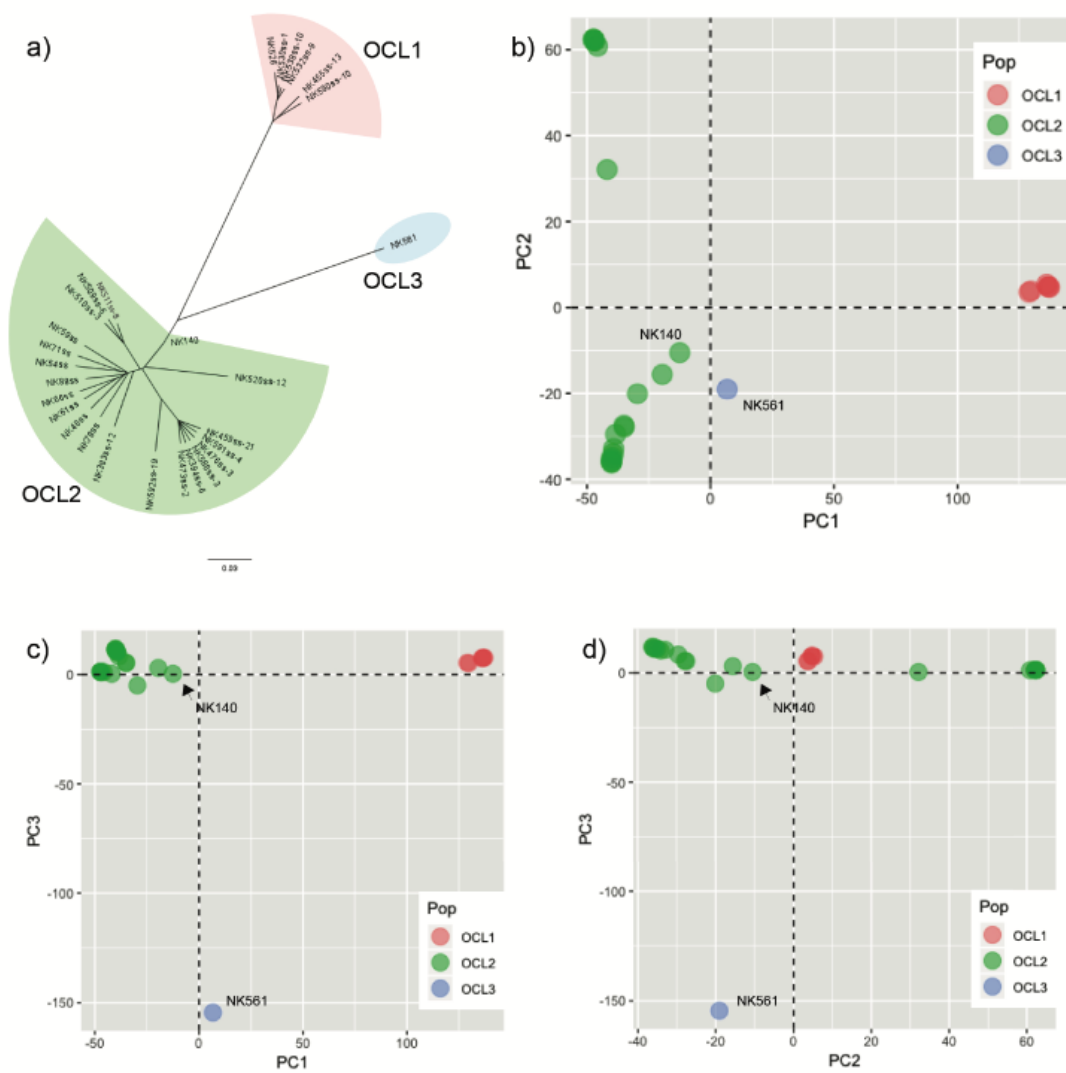


**Fig.S7** Population structure among the samples belonging to *Ophiocordyceps camponoti-leonardi*. a) Neighbor-joining tree based on an alignment of single nucleotide polymorphisms (SNPs) and using the F84 distance. b) – d) Principal component analyses (PCA) based on SNPs.

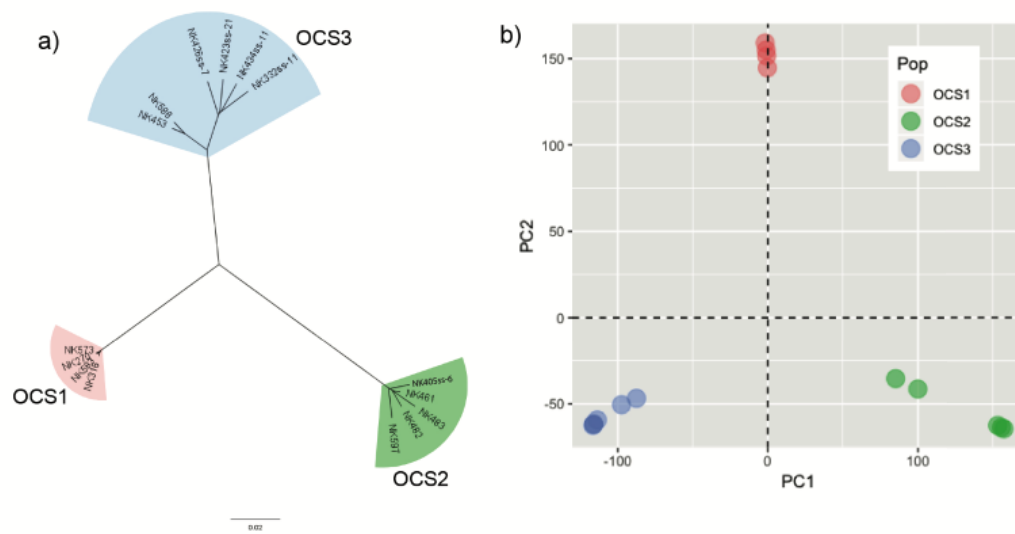


**Fig.S8** Population structure among the samples belonging to *Ophiocordyceps camponoti-saundersi*. a) Neighbor-joining tree based on an alignment of single nucleotide polymorphisms (SNPs) using the F84 distance. b) A principal component analysis (PCA) based on SNPs.

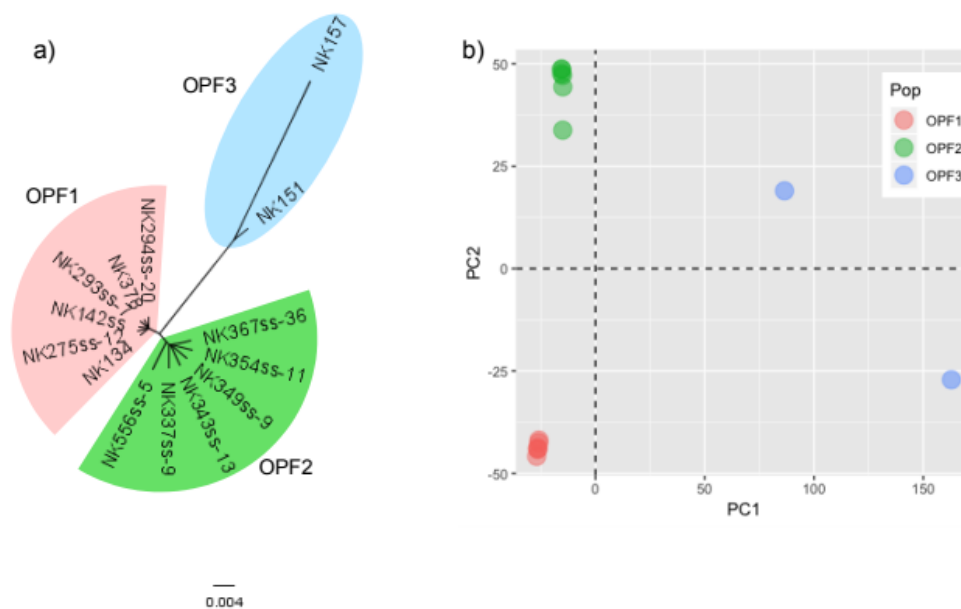


**Fig.S9** Population structure among the samples belonging to *Ophiocordyceps polyrhachis-furcata*. a) Neighbor-joining tree from based on an alignment of single nucleotide polymorphisms (SNPs) and using the F84 distance. b) A principal component analysis (PCA) based on SNPs.

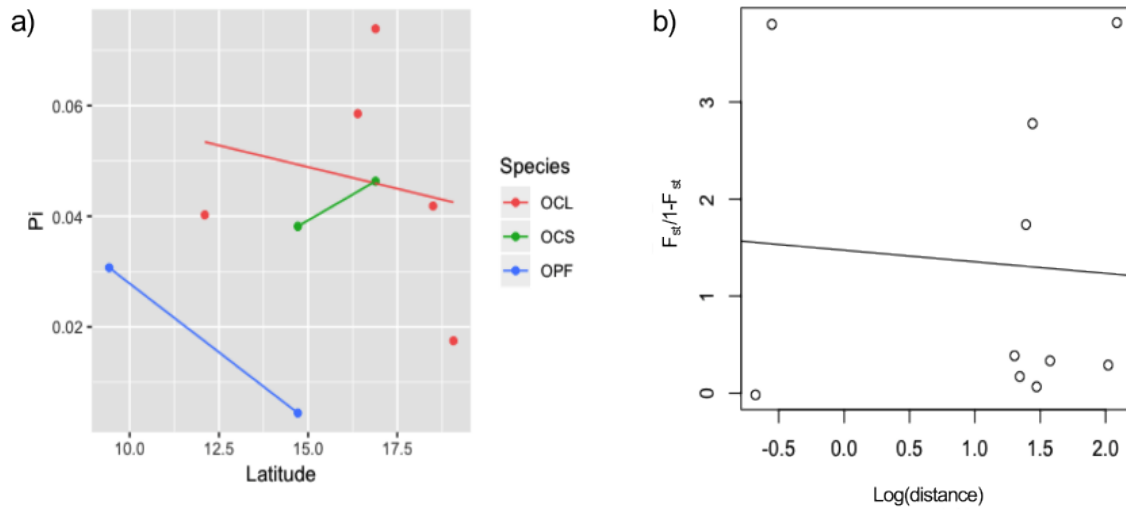


**Fig.S10** a) Correlation between nucleotide diversity ( $P_i$ ) per site and per species and the sampling site latitude (OCL = *Ophiocordyceps camponoti-leonardi*, OCS = *O. camponoti-saundersi*, OPF = *O. polyrhachis-furcata*). b) Correlation between genetic dissimilarity between sampling sites of *O. camponoti-leonardi* ( $F_{st}/1-F_{st}$ ) and the log distance between sites.

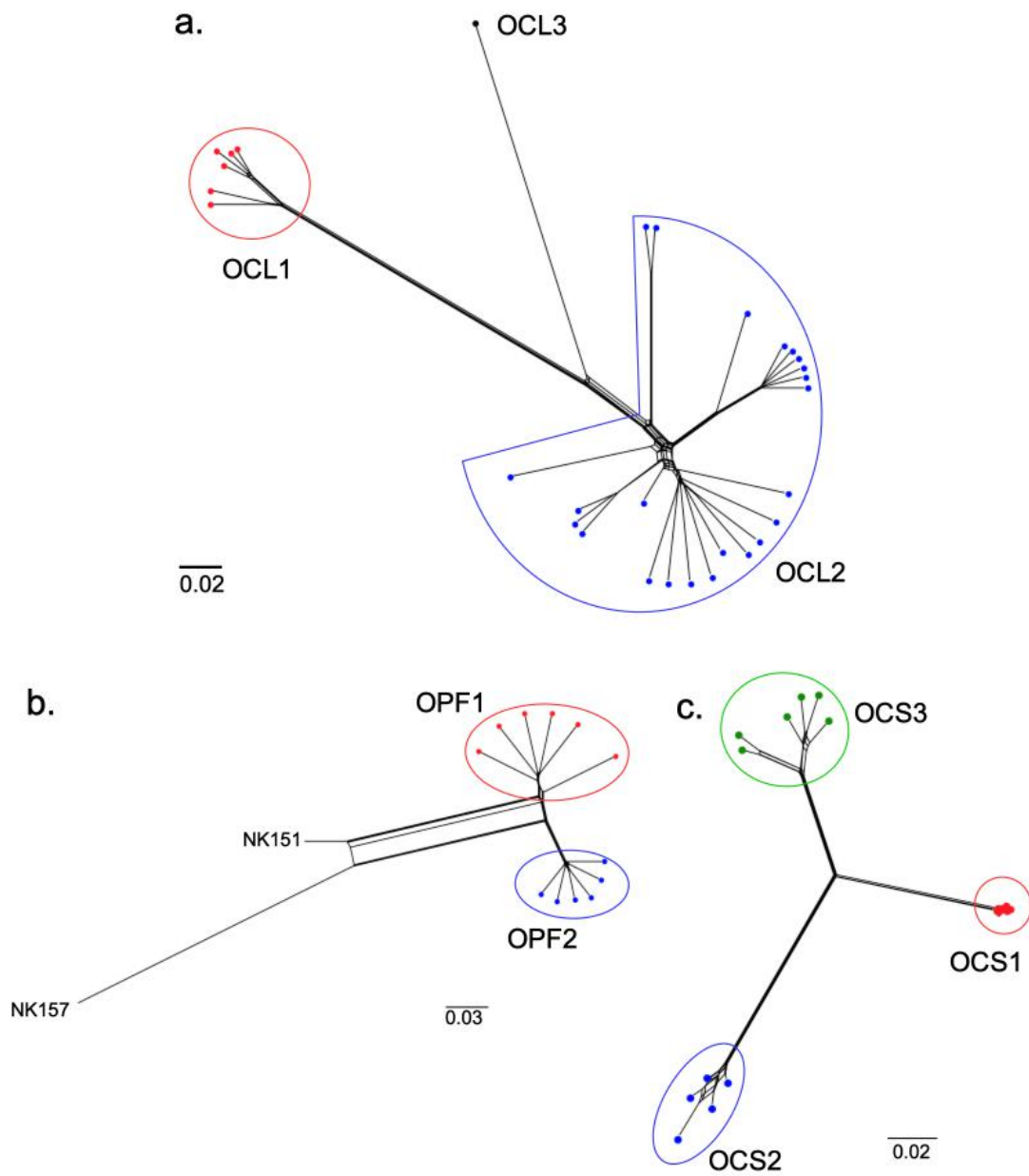


**Fig.S11** Neighbor-net phylogenetic networks for a) *Ophiocordyceps camponoti-leonardi*, b) *O. polyrhachis-furcata* and c) *O. camponoti-saundersi*.

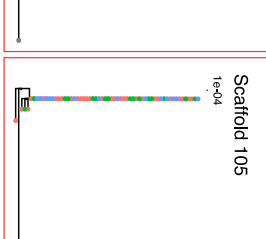
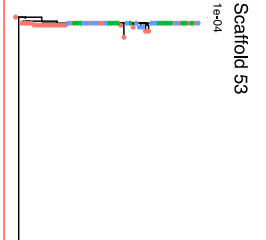
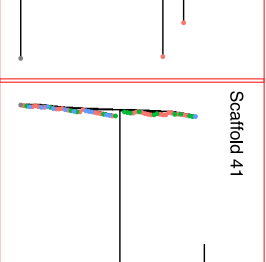
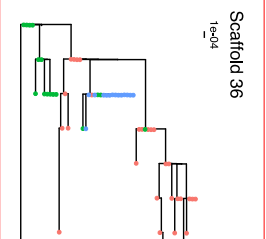
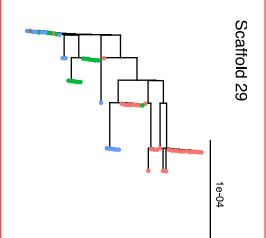
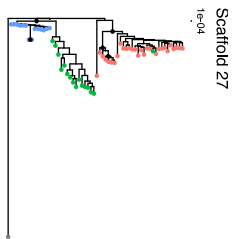
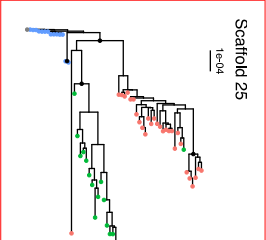
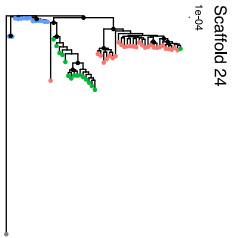
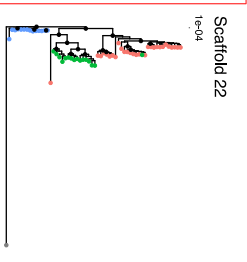
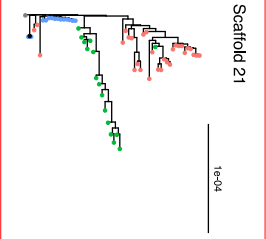
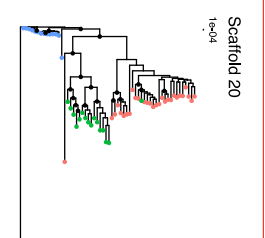
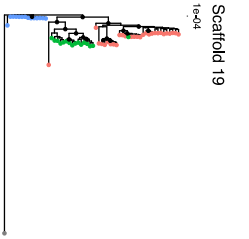
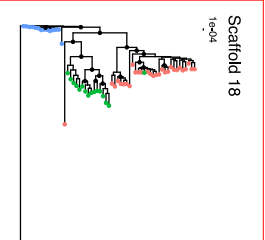
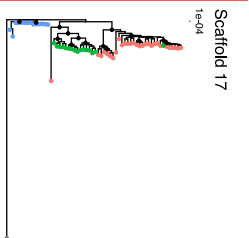
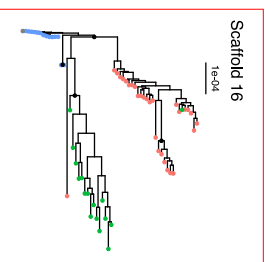
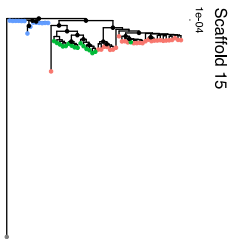
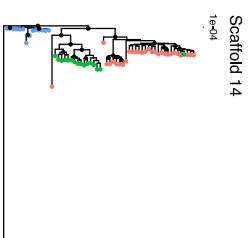
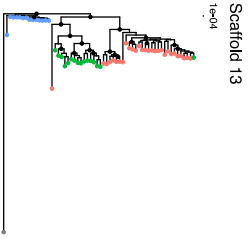
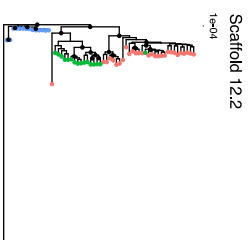
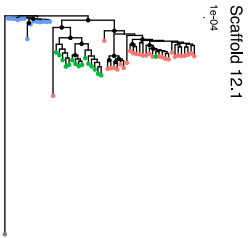
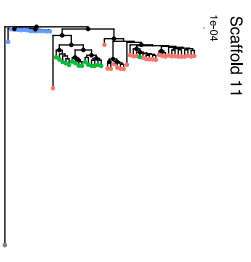
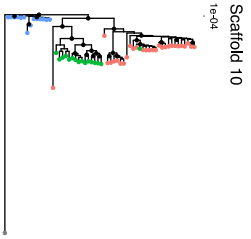
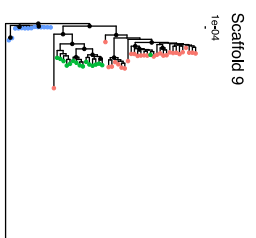
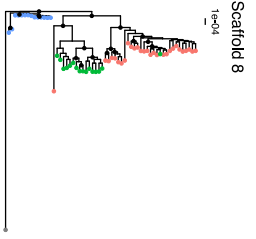
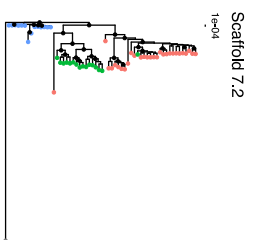
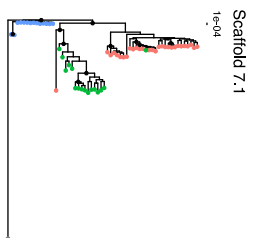
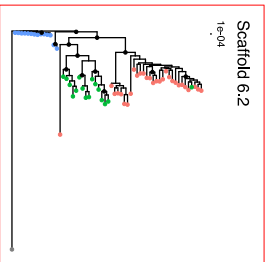
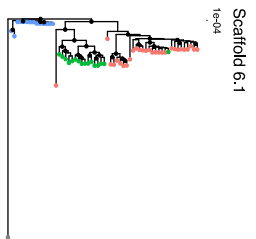


**Table S1** : Fungal isolates used in this study (BCC = Biotec Culture Collection Accession Number, BBH = Biotec Bangkok Herbarium accession number).

<b>Isolate</b>	<b>Isolation method</b>	<b>Ant host</b>	<b>Site</b>	<b>Province</b>	<b>BCC</b>	<b>BBH</b>	<b>BioSample</b>
NK122ss	single spore	<i>Colobopsis leonardi</i>	Halabala Wildlife Sanctuary	Narathiwat	69099	37954	SAMN11321611
NK134	multiple spores	<i>Polyrhachis furcata</i>	Khao Yai National Park	Nakhon Ratchasima	70388	38294	SAMN11321612
NK140	multiple spores	<i>Colobopsis leonardi</i>	Khao Yai National Park	Nakhon Ratchasima	70397	38300	SAMN11321613
NK270	multiple spores	<i>Colobopsis saundersi</i>	Khao Yai National Park	Nakhon Ratchasima	75911	39875	SAMN11321614
NK293ss-7	single spore	<i>Polyrhachis furcata</i>	Khao Yai National Park	Nakhon Ratchasima	75920	39883	SAMN11321615
NK294ss-20	single spore	<i>Polyrhachis furcata</i>	Khao Yai National Park	Nakhon Ratchasima	-	41439	SAMN11321616
NK332ss-1	single spore	<i>Colobopsis saundersi</i>	Khao Yai National Park	Nakhon Ratchasima	78437	39890	SAMN11321617
NK337/ss-9	single spore	<i>Polyrhachis furcata</i>	Khlong Nakha Wildlife Sanctuary	Ranong	79284	41466	SAMN11321618
NK343ss-13	single spore	<i>Polyrhachis furcata</i>	Khlong Nakha Wildlife Sanctuary	Ranong	78443	41472	SAMN11321619
NK349ss-9	single spore	<i>Polyrhachis furcata</i>	Khlong Nakha Wildlife Sanctuary	Ranong	78445	41478	SAMN11321620
NK354ss-11	single spore	<i>Polyrhachis furcata</i>	Khlong Nakha Wildlife Sanctuary	Ranong	78446	41483	SAMN11321621
NK367/ss-36	single spore	<i>Polyrhachis furcata</i>	Khlong Nakha Wildlife Sanctuary	Ranong	78449	41496	SAMN11321622
NK378	multiple spores	<i>Polyrhachis furcata</i>	Khao Yai National Park	Nakhon Ratchasima	79295	41503	SAMN11321623
NK383ss-12	single spore	<i>Colobopsis leonardi</i>	Phu Khiao Wildlife Sanctuary	Chaiyaphum	79300	41508	SAMN11321624
NK394ss-6	single spore	<i>Colobopsis leonardi</i>	Phu Khiao Wildlife Sanctuary	Chaiyaphum	79306	41519	SAMN11321625
NK48ss	single spore	<i>Colobopsis leonardi</i>	Ko Chang Island	Trat	68537	37537	SAMN11321626
NK54ss	single spore	<i>Colobopsis leonardi</i>	Ko Chang Island	Trat	68541	37541	SAMN11321627
NK59ss	single spore	<i>Colobopsis leonardi</i>	Ko Chang Island	Trat	68545	37543	SAMN11321628
NK61ss	single spore	<i>Colobopsis leonardi</i>	Ko Chang Island	Trat	68548	37545	SAMN11321629
NK66ss	single spore	<i>Colobopsis leonardi</i>	Ko Chang Island	Trat	68551	37548	SAMN11321630
NK71ss	single spore	<i>Colobopsis leonardi</i>	Ko Chang Island	Trat	69073	38283	SAMN11321631
NK78ss	single spore	<i>Colobopsis leonardi</i>	Ko Chang Island	Trat	69077	37944	SAMN11321632
NK88ss	single spore	<i>Colobopsis leonardi</i>	Ko Chang Island	Trat	69080	37555	SAMN11321633
NK459ss-21	single spore	<i>Colobopsis leonardi</i>	Nam Nao National Park	Petchabun	80028	41583	SAMN11321634
NK476ss-3	single spore	<i>Colobopsis leonardi</i>	Nam Nao National Park	Petchabun	80038	41600	SAMN11321635
NK509ss-6	single spore	<i>Colobopsis leonardi</i>	Doi Inthanon National Park	Chiang Mai	80043	41633	SAMN11321636

NK510ss-3	single spore	<i>Colobopsis leonardi</i>	Doi Inthanon National Park	Chiang Mai	80366	41634	SAMN11321637
NK511ss-8	single spore	<i>Colobopsis leonardi</i>	Doi Inthanon National Park	Chiang Mai	80369	41635	SAMN07662903
NK526	multiple spores	<i>Colobopsis leonardi</i>	Ban Huay Baba	Chiang Mai	80379	42812	SAMN11321638
NK532ss-9	single spore	<i>Colobopsis leonardi</i>	Ban Huay Baba	Chiang Mai	80044	42818	SAMN11321639
NK455ss-8	single spore	<i>Colobopsis leonardi</i>	Nam Nao National Park	Petchabun	80360	41580	SAMN11321640
NK473ss-2	single spore	<i>Colobopsis leonardi</i>	Nam Nao National Park	Petchabun	80614	41597	SAMN11321641
NK520ss-12	single spore	<i>Colobopsis leonardi</i>	Doi Inthanon National Park	Chiang Mai	80377	41644	SAMN11321642
NK530ss-1	single spore	<i>Colobopsis leonardi</i>	Ban Huay Baba	Chiang Mai	80380	42816	SAMN11321643
NK538ss-10	single spore	<i>Colobopsis leonardi</i>	Ban Huay Baba	Chiang Mai	80045	42824	SAMN11321644
NK561	multiple spores	<i>Colobopsis leonardi</i>	Khao Luang National Park	Nakhonsithamarat	80621	41657	SAMN11321645
NK588ss-3	single spore	<i>Colobopsis leonardi</i>	Khao Luang National Park	Petchabun	84568	42855	SAMN11321646
NK590ss-10	single spore	<i>Colobopsis leonardi</i>	Khao Luang National Park	Petchabun	84571	42857	SAMN11321647
NK591ss-4	single spore	<i>Colobopsis leonardi</i>	Khao Luang National Park	Petchabun	84581	42858	SAMN11321648
NK592ss-19	single spore	<i>Colobopsis leonardi</i>	Khao Luang National Park	Petchabun	-	42859	SAMN11321649
NK316	multiple spores	<i>Colobopsis saundersi</i>	Khao Yai National Park	Nakhon Ratchasima	-	39888	SAMN11321650
NK405ss-6	single spore	<i>Colobopsis saundersi</i>	Phu Khiao Wildlife Sanctuary	Chaiyaphum	79314	41530	SAMN07662932
NK423ss-21	single spore	<i>Colobopsis saundersi</i>	Khao Yai National Park	Nakhon Ratchasima	79321	41548	SAMN11321651
NK426ss-7	single spore	<i>Colobopsis saundersi</i>	Khao Yai National Park	Nakhon Ratchasima	79326	41551	SAMN11321652
NK434ss-11	single spore	<i>Colobopsis saundersi</i>	Khao Yai National Park	Nakhon Ratchasima	79331	41559	SAMN11321653
NK461	multiple spores	<i>Colobopsis saundersi</i>	Nam Nao National Park	Petchabun	-	41585	SAMN11321654
NK453	multiple spores	<i>Colobopsis saundersi</i>	Nam Nao National Park	Petchabun	-	41578	SAMN11321655
NK482	multiple spores	<i>Colobopsis saundersi</i>	Nam Nao National Park	Petchabun	80039	41606	SAMN11321656
NK483	multiple spores	<i>Colobopsis saundersi</i>	Nam Nao National Park	Petchabun	80040	41607	SAMN11321657
NK573	multiple spores	<i>Colobopsis saundersi</i>	Khao Yai National Park	Nakhon Ratchasima	82852	42840	SAMN11321658
NK583	multiple spores	<i>Colobopsis saundersi</i>	Khao Yai National Park	Nakhon Ratchasima	84565	42850	SAMN11321659
NK586	multiple spores	<i>Colobopsis saundersi</i>	Nam Nao National Park	Petchabun	-	42853	SAMN11321660
NK597	multiple spores	<i>Colobopsis saundersi</i>	Nam Nao National Park	Petchabun	-	42864	SAMN11321661
NK604	multiple spores	<i>Colobopsis saundersi</i>	Nam Nao National Park	Petchabun	84591	42871	SAMN11321662
NK142ss	single spore	<i>Polyrhachis furcata</i>	Khao Yai National Park	Nakhon Ratchasima	-	38301	SAMN11321663
NK275ss-12	single spore	<i>Polyrhachis furcata</i>	Khao Yai National Park	Nakhon Ratchasima	75913	39877	SAMN11321664

NK151	multiple spores	<i>Polyrhachis furcata</i>	Khlong Naka Wildlife Sanctuary	Ranong	71355	38599	SAMN11321665
NK157	multiple spores	<i>Polyrhachis furcata</i>	Khlong Naka Wildlife Sanctuary	Ranong	70665	38304	SAMN11321666
NK556ss-5	single spore	<i>Polyrhachis furcata</i>	Khao Luang National Park	Nakhonsithammarat	-	41652	SAMN11321667

**Table S2:** Genetic diversity per scaffold in *Ophiocordyceps unilateralis sensu lato*

<b>Scaffold</b>	<b>Length</b>	<b>SNPs Number</b>	<b>Pi</b>
1	5280523	136209	0.034
2.1	818828	24837	0.035
2.2	3902607	55058	0.032
3	2977708	19974	0.037
4	2824012	33938	0.038
5	2463813	14234	0.035
6.1	4344696	102669	0.032
6.2	247174	4663	0.046
7.1	407820	3955	0.000
7.2	4080701	49613	0.032
8	3328657	15513	0.033
9	1794465	17459	0.040
10	1211063	33165	0.034
11	1131199	32372	0.032
12.1	386211	10282	0.000
12.2	604937	16862	0.032
13	939609	18870	0.035
14	963256	24241	0.034
15	795048	16431	0.033
16	630955	1058	0.043
17	583368	12928	0.034
18	594624	8781	0.031
19	433702	9584	0.033
20	376207	9947	0.032
21	373426	113	0.000
22	342176	9096	0.043
24	164406	4377	0.036
25	156640	500	0.066
27	99302	1468	0.031
29	50804	17	0.015
36	7493	19	0.000
41	11136	1	0.000
53	1236	23	0.000
105	8111	7	0.000

**Table S3:** Genetic diversity by site and by species: OCL = *Ophiocordyceps camponoti-leonardi*, OCS = *O. camponoti-saundersi*, OPF = *O. polyrhachis-furcata*. Pi = nucleotide diversity.

Sampling Site	Province	Latitude	Species		
			OCL	OCS	OPF
Ban Huai Baba	Chiang Mai	19.070	0.0056	-	-
Doi Inthanon National Park	Chiang Mai	18.498	0.0138	-	-
Nam Nao National Park	Phetchabul	16.887	0.0225	0.0121	-
Phu Khiao Wildlife Sanctuary	Chaiyaphum	16.390	0.0195	-(one sample)	-
Khao Yai National Park	Nakhon Ratchasima	14.712	-(one sample)	0.0108	0.0014
Ko Chang Island	Trad	12.103	0.0129	-	-
Khlong Nakha Wildlife Sanctuary	Chumphon	9.423	-	-	0.0097
Khao Luang National Park	Nakhon Sithamarat	8.373	-(one sample)	-	-(one sample)
Hala Bala Wildlife Sanctuary	Narathiwat	5.928	-	-	-

Table S4. Results of PHI tests of signature of recombination. (OCL = *Ophiocordyceps camponoti-leonardi*, OCS = *O. camponoti-saundersi*, OPF = *O. polyrhachis-furcata*) NAs indicate lack of sufficient informative sites.

Scaffold	All	OCL	OCL1	OCL2	OCS	OCS1	OCS2	OCS3	OPF	OPF1	OPF2
scaffold1	0.000	0.000	0.000	0.000	0.000	0.000	0.000	0.000	0.000	0.000	0.000
scaffold2.1	0.000	0.000	0.000	0.000	0.000	0.000	0.000	0.000	0.000	0.000	0.000
scaffold2.2	0.000	0.000	0.000	0.000	0.000	0.000	0.000	0.000	0.000	0.000	0.000
scaffold3	0.000	0.000	0.000	0.000	0.000	0.000	0.000	0.000	0.000	0.000	0.000
scaffold4	0.000	0.000	0.000	0.000	0.000	0.000	0.000	0.000	0.000	0.000	0.000
scaffold5	0.000	0.000	0.000	0.000	0.000	0.000	0.000	0.000	0.000	0.658	1.000
scaffold6.1	0.000	0.000	0.000	0.000	0.000	0.000	0.000	0.000	0.000	0.000	0.000
scaffold6.2	0.000	0.000	0.000	0.000	0.000	0.000	0.000	0.000	0.000	1.000	1.000
scaffold7.1	0.000	0.000	0.000	0.000	0.000	0.000	0.000	0.000	1.000	1.000	1.000
scaffold7.2	0.000	0.000	0.000	0.000	0.000	0.000	0.000	0.000	0.000	0.000	0.000
scaffold8	0.000	0.000	0.000	0.000	0.000	0.000	0.000	0.000	0.000	0.000	0.000
scaffold9	0.000	0.000	0.000	0.000	0.000	0.000	0.000	0.000	0.000	0.000	0.000
scaffold10	0.000	0.000	0.000	0.000	0.000	0.000	0.000	0.000	0.000	0.000	0.000
scaffold11	0.000	0.000	0.000	0.000	0.000	0.000	0.000	0.000	0.000	0.000	0.000
scaffold12.1	0.000	0.000	0.000	0.000	0.000	0.000	0.000	0.000	0.000	0.000	1.000
scaffold12.2	0.000	0.000	0.000	0.000	0.000	0.000	0.000	0.000	0.658	0.000	0.000
scaffold13	0.000	0.000	0.000	0.000	0.000	0.000	0.000	0.000	0.000	0.000	0.000
scaffold14	0.000	0.000	0.000	0.000	0.000	0.000	0.000	0.000	0.000	0.000	0.000
scaffold15	0.000	0.000	0.000	0.000	0.000	0.000	0.000	0.000	0.000	0.000	0.000
scaffold16	0.000	0.000	0.000	0.000	0.000	0.000	0.000	0.000	1.000	NA	NA
scaffold17	0.000	0.000	0.000	0.000	0.000	0.000	0.000	0.000	0.000	0.000	0.000
scaffold18	0.000	0.000	0.000	0.000	0.000	0.000	0.000	0.000	0.000	0.000	0.000
scaffold19	0.000	0.000	0.000	0.000	0.000	0.000	0.000	0.000	1.000	0.000	1.000
scaffold20	0.000	0.000	0.000	0.000	0.000	0.000	0.000	0.000	0.000	0.000	0.987
scaffold21	0.987	0.000	1.000	0.000	1.000	1.000	1.000	1.000	1.000	NA	NA
scaffold22	0.000	0.000	0.000	0.000	0.000	0.000	0.000	0.000	0.000	0.000	0.329
scaffold24	0.000	0.000	0.000	0.000	0.000	0.000	0.000	0.000	1.000	1.000	1.000
scaffold25	0.000	0.000	1.000	0.000	0.000	0.000	1.000	0.000	1.000	NA	1.000
scaffold27	0.000	0.000	1.000	0.000	0.000	0.000	0.000	0.000	1.000	1.000	1.000



**Table S5: The observed, expected number of homozygous sites, total number of SNPs and inbreeding coefficient for the diploid samples.**

<b>Samples</b>	<b>Species</b>	<b>Observed</b>	<b>Expected</b>	<b>Total</b>	<b>F coefficient</b>
NK134	<i>O. polyrhachis-furcata</i>	687858	596600	687858	1
NK140	<i>O. camponoti-leonardi</i>	640930	560000	642118	0.9855
NK270	<i>O. camponoti-saundersi</i>	645429	561400	645447	0.9998
NK378	<i>O. polyrhachis-furcata</i>	687619	596400	687620	1
NK526	<i>O. camponoti-leonardi</i>	663027	575500	663042	0.9998
NK561	<i>O. camponoti-leonardi</i>	663418	576800	663422	1
NK316	<i>O. camponoti-saundersi</i>	646450	563200	646468	0.9998
NK461	<i>O. camponoti-saundersi</i>	640107	558300	640151	0.9995
NK453	<i>O. camponoti-saundersi</i>	561257	487900	561296	0.9995
NK482	<i>O. camponoti-saundersi</i>	453036	391900	453065	0.9995
NK483	<i>O. camponoti-saundersi</i>	643876	560500	643892	0.9998
NK573	<i>O. camponoti-saundersi</i>	647183	562900	647204	0.9998
NK583	<i>O. camponoti-saundersi</i>	646163	562200	646175	0.9999
NK586	<i>O. camponoti-saundersi</i>	646587	562700	646629	0.9995
NK597	<i>O. camponoti-saundersi</i>	644848	561400	644867	0.9998
NK604	<i>O. camponoti-leonardi</i>	670466	582300	670481	0.9998
NK151	<i>O. polyrhachis-furcata</i>	686833	595700	686833	1
NK157	<i>O. polyrhachis-furcata</i>	685814	594800	685816	1